BRNO UNIVERSITY OF TECHNOLOGY

Faculty of Electrical Engineering
and Communication

MASTER'S THESIS

Brno, 2017 Bc. Petra Novotná

BRNO UNIVERSITY OF TECHNOLOGY
VYSOKÉ UČENÍ TECHNICKÉ V BRNĚ

FACULTY OF ELECTRICAL ENGINEERING AND COMMUNICATION
FAKULTA ELEKTROTECHNIKY
A KOMUNIKAČNÍCH TECHNOLOGIÍ

DEPARTMENT OF BIOMEDICAL ENGINEERING
ÚSTAV BIOMEDICÍNSKÉHO INŽENÝRSTVÍ

ANALYSIS OF HIGH-FREQUENCY ECG AND MECHANO-ELECTRIC COUPLING IN ISOLATED HEART
ANALÝZA VYSOKOFREKVENČNÍCH EKG SIGNÁLŮ A MECHANO-ELEKTRICKÉ VAZBY U IZOLOVANÉHO SRDCE

MASTER'S THESIS
DIPLOMOVÁ PRÁCE

AUTHOR — **Bc. Petra Novotná**
AUTOR PRÁCE

SUPERVISOR — **Ing. Jakub Hejč**
VEDOUCÍ PRÁCE

BRNO 2017

BRNO UNIVERSITY OF TECHNOLOGY
FACULTY OF ELECTRICAL ENGINEERING AND COMMUNICATION

Master's Thesis

Master's study field **Biomedical Engineering and Bioinformatics**
Department of Biomedical Engineering

Student: Bc. Petra Novotná ***ID:*** 154643
Year of study: 2 ***Academic year:*** 2016/17

TITLE OF THESIS:

Analysis of High-Frequency ECG and Mechano-Electric Coupling in Isolated Heart

INSTRUCTION:

1) Present literature research on methods of multi-channel, and high-frequency ECG measurement and analysis. Get familiar with experimental signal database containing unipolar electrograms, continuous blood pressure, and volumetric flow data measured on isolated hearts. 2) Perform a critical analysis on provided data. Choose suitable frequency bands for high-frequency ECG analysis. Choose suitable parameters for assessment and evaluation of the relationship between isolated heart hemodynamics and high-frequency ECG. 3) Create an algorithm for automatic detection of selected cardiovascular parameters. 4) Process measured parameters with appropriate statistical methods. Evaluate the impact of alteration in heart hemodynamics on high-frequency ECG parameters. 5) Discuss the results of statistical analysis in detail.

REFERENCE:

[1] TRÄGARDH, E., SCHLEGEL, T. T. High-frequency QRS electrocardiogram. Clinical Physiology and Functional Imaging, 2007, vol. 27:4, s. 197-204.

[2] JURAK, P., HALAMEK, J., PLESINGER, F., et al. An Additional Marker of Ventricular Dyssynchrony. Computing in Cardiology Conference 2015, 2015, vol. 42, s. 77–80.

Assigment deadline: 6. 2. 2017 ***Submission deadline:*** 19.5.2017

Head of thesis: Ing. Jakub Hejč
Consultant: José Millet Roig

prof. Ing. Ivo Provazník, Ph.D.
Subject Council chairman

ABSTRACT

This master's thesis deals with the analysis of high frequency ECG from the perspective of mechano-electric coupling in isolated rabbit heart. The first part of this thesis is the literature review considering given thematics. It contains information about formation and genesis of ECG and action potential at the chemical and electric level, mechano-electric coupling. The thesis contains the chapter about signal averaging as the technique for gaining the signal-to-noise ratio when analysing HF ECG. In the part of practical application is the knowledge applied to the long recordings of isolated rabbit heart's ECG. There is the description of perfusion system according to Neely included. The realisation consists of data from 15 isolated rabbit hearts to be analysed and explored for the presence of system's reaction to the change of input parameters (preload, afterload) for the case of pressure-volume data. The results have been connected to the similar ones from HF ECG and altogether they create the description of mechano-electric coupling of heart. The reuslts have been statistically tested and evaluated.

KEYWORDS

ECG, HF analysis, isolated rabbit heart, signal averaging, mechano-electric coupling, perfusion system, Langendorff, Neely, experimental ECG recordings

ABSTRAKT

Tato magisterská práce se zabývá analýzou vysokofrekvenčních složek záznamu EKG z pohledu mechano-elektrické vazby u izolovaného králičího srdce. První částí této práce je literární rešerše na zadané téma zahrnující informace o vzniku a šíření akčního potenciálu na chemické i elektrické úrovní i mechano-elektrické zpětné vazbě. Dále práce obsahuje kapitolu zabývající se tématikou průměrování signálu jako techniky ke zvýšení poměru signál-šum při analýze vysokofrekvenčních složek. V praktické části práce jsou získané poznatky aplikovány na dlouhé záznamy EKG z izolovaných králičích srdcí. Zahrnut je popis perfuzního systému podle Neelyho a jeho užití při experimentech. V realizaci byla data z 15 izolovaných králičích srdcí podrobeno analýze zkoumající přítomnost reakce systému na změnu vstupních parametrů (afterloadu a preploadu) v případě tlakově objemových dat. Výsledky byly vztaženy ke stejně získaným hodnotám z HF ECG. Dohromady tvoří popis mechano-elektriké reakce srdce na hemodynamické podněty. Výsledky byly statistisky testovány a vyhodnoceny.

KLÍČOVÁ SLOVA

EKG, VF analýza, izolované králičí srdce, průměrování signálu, mechano-elektrická vazba, perfuzní systém, Langendorff, Neely, experimentální EKG záznamy

NOVOTNÁ, Petra *ANALYSIS OF HIGH-FREQUENCY ECG AND MECHANO- ELECTRIC COUPLING IN ISOLATED HEART*: master's thesis. Brno: Brno University of Technology, Faculty of Electrical Engineering and Communication, Department of Biomedical Engineering, 2017. 95 p. Supervised by Ing. Jakub Hejč

DECLARATION

I declare that I have written my master's thesis on the theme of "ANALYSIS OF HIGH-FREQUENCY ECG AND MECHANO- ELECTRIC COUPLING IN ISOLATED HEART" independently, under the guidance of the master's thesis supervisor and using the technical literature and other sources of information which are all quoted in the thesis and detailed in the list of literature at the end of the thesis.

As the author of the master's thesis I furthermore declare that, as regards the creation of this master's thesis, I have not infringed any copyright. In particular, I have not unlawfully encroached on anyone's personal and/or ownership rights and I am fully aware of the consequences in the case of breaking Regulation § 11 and the following of the Copyright Act No 121/2000 Sb., and of the rights related to intellectual property right and changes in some Acts (Intellectual Property Act) and formulated in later regulations, inclusive of the possible consequences resulting from the provisions of Criminal Act No 40/2009 Sb., Section 2, Head VI, Part 4.

Brno ....

(author's signature)

ACKNOWLEDGEMENT

I would like to thank my supervisor, mister Ing. Jakub Hejč, for his leading, advices, time, patience and effort he had for me through the whole year. I would also like to thank my family for their never-ending support.

Brno ....

(author's signature)

CONTENTS

LIST OF FIGURES

LIST OF TABLES

INTRODUCTION

The heart is, has always been and surely will be a fascinating organ which works all along through our lives. Its journey starts with the first differentiation of cardiocytes and ends with the last heartbeat. We do not have to concentrate on the handling of it and it still fulfils its mission for us, or any other living creature. Except for our parents when they won't let us go to a party, they just don't have a heart. Truly.

It is natural that the heart has been the subject of research since the beginning of the history of mankind and it is seriously fascinating that we still do not understand it completely.

The electrocardiography and its outcome, electrocardiogram (ECG), are the way how to record the heart's electrical activity as a chronological order of deflections of potentials. It has been firstly used as a clinical tool by Willem Einthoven at the beginning of the 20th century. The whole history of understanding the ECG is very interesting, but one of the major changes happened with the arrival of computing technologies. Since then, ECG has become a tool without which would have current science and medicine very hard times especially in diagnostics, monitoring of treatment.

This master's thesis has its purpose in the high-frequency analysis of high resolution ECG signals got from experiments performed on isolated hearts from New Zealand rabbits. The methodology is the merge of facts known about human and rabbit heart. The methods of analysis are mainly very similar to those used for analysis of ECG from human hearts however they need to be applied with respect to the rabbit hearts properties and behaviour.

The first, literature review part, of the master's thesis deals with the problematics on the theoretical base. There are mentioned the principles of heart's working, the chemical essence of it, the ways how to record the ECG from the body surface and an introduction to the high-frequency analysis. The second part aims at the practical usage of gained knowledge. It outlines the algorithm of the analysis and covers the details of applications and their pros or cons.

LITERATURE REVIEW

1 HEART AND ELECTROCARDIOGRAM

The heart is a necessary organ working practically from the third week of prenatal evolution until the end of life, which is magnificently metabolically demanding. The function of the heart can be described in two ways - as mechanical type, when the heart is looked at as volume pump, and as electrical converter of action potential. There is a very tight connection between both types of work named *excitation-contraction connection* and *mechano-electric couppling*.

The pumping mechanism contains two units, each assembled from atrium and ventriculus. Those units are mutually connected, but separated by valves. They have the same rhythm and so the same minute yield of blood. Both, body and pulmonary, circulatory systems start and end here. The heart disposes of amount of regulatory mechanisms, because of which it can adapt to the changing character of working conditions and ran quickly and effectively respond to organism requirements.

Cardiac conduction system is made of cells, which specialise on the creation and propagation of the electrical impulse. The run starts in the sinoatrial node (SAN), where under normal conditions the pulse is formed. The preferential atrial paths lead the pulse to the atrioventricular node (AVN). There, in the case of malfunction of the SAN, takes over the service of being the pacemaker. Through the His bundle and both of it's Tawara branches the puls gets to the Purkinje fibers, which excite the myocardium of ventricles. In it, the excitation is propagated from the inside to the outside and from the apex to the base of the heart. The process of the excitation, the potential differences, is able to be observed thanks to the electrocardiogram (ECG).

Normal process of the ECG with its features can be seen at the Fig. 2.1.

2 FORMATION OF THE ECG

ECG as an information source refers to the heart's position, heart rate variability, origin and transmission of the impulses and the repolarisation. It also informs about the pathological conditions in the heart considering these actions. [1]

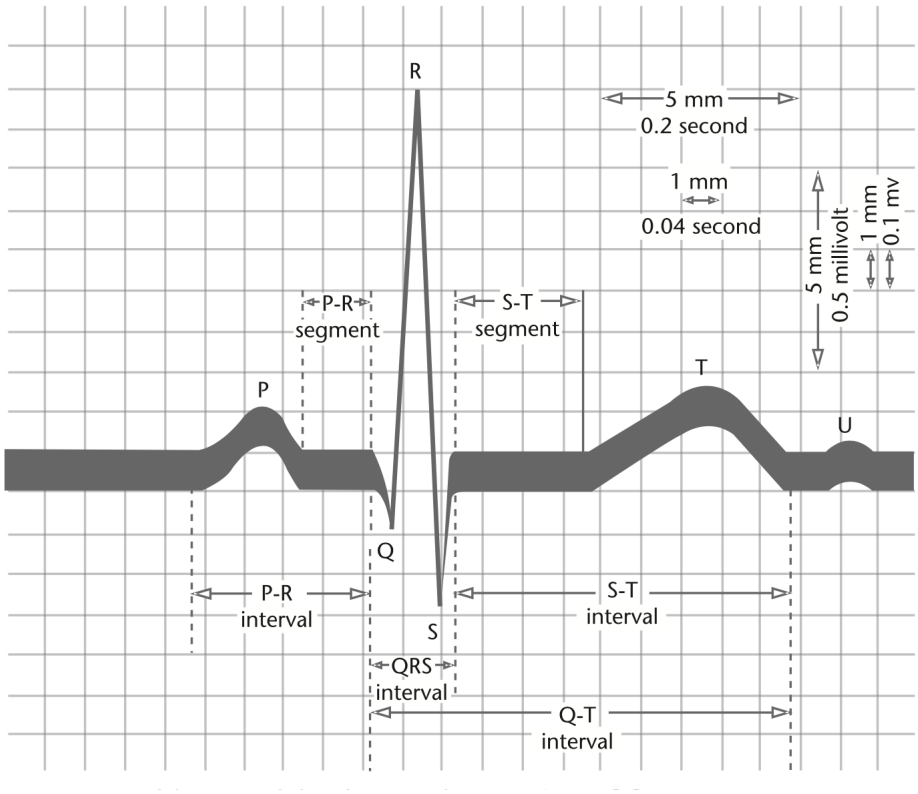

Fig. 2.1: Normal features of the electrocardiogram.

2.1 Action potential

The migration of the excitatory front through the heart muscle stimulates the potential differences at the interface between stimulated and non-stimulated myocardium. The principle of propagated activity is in the cells grouped together by gap junctions. Those cells, in the normal healthy heart, have almost none or very low resistance. Because of that, the activity is propagated easily, uniformly and between neighbouring cells that are still and rest. The cell's membrane potential is changed from positive to negative. This behaviour is called syncytial. In the ECG we observe the movement of the wavefront though the heart and as a whole we call it the depolarisation.

The cardiac action potential is a short-lasting event in which the cell's membrane potential changes which leads to the contraction of the heart. The membrane changes are the results of the ion movements between the interior and exterior of the cell. There will be described two types of action potential (AP). [2]

The first one is the AP of the peacemaker cells. These cells are the participants of the electrical conduction system of the heart and provide the electrical activation. They do not need their neighbour cells to propagate the impulse, this action happens automatically and the cells do it all by themselves. The ion exchange on the membrane is executed by the system of voltage gated channels. The main ions involved in the exchange are calcium (Ca^{2+}) with its own steady potential at +123 mV, sodium (Na^{+}) which has the steady potential at +67 mV and potassium (K^{+}) with the steady potential at -92 mV.

At the beginning, the cell's membrane is found at its basic potential. It can not be called the *rest* potential, because there really is not one. The membrane's potential starts at -60 mV at the moment, where only sodium channels are opened and Na^{+} is entering the cell by its concentration gradient. Because of the positive character of sodium ions, the membrane potential starts rising and reaches roughly -40 mV. This level of potential is called the threshold. Crossing this threshold causes the opening of calcium voltage gated channels. The Ca^{2+} ions start leaking in the cell and become the major ions for which the membrane is permeable. This action causes the level of membrane potential to rise rapidly towards the steady potential of calcium. At the level of +10 mV the polarity of membrane is switched which induce the closing of the calcium channels and opening the potassium channels. The K^{+} ions start departing the cell according to theirs concentration gradient and become the dominant ions of the exchanging process. Because of the K^{+} being the major ions, the membrane potential level endeavours for reaching the potassium steady potential at -92 mV. This progression stops at -60 mV, where the potassium channels are shut down and again, only Na^{+} ions are entering the cell. The whole

cycle of peacemaker cells is called *slow* because of its unhurried growth in the socalled *zero* state.

The second type of the AP that will be described is the AP of cardiac myocytes, which is connected to the mechanical activation of the heart. The trigger of the heart muscle contraction is calcium. The depolarisation commences at the level of -90 mV. The K^+ ions are leaving the cell naturally up to the membrane potential level of -70 mV. At that moment the Na^+ ions start entering the cell in accordance with their concentration gradient. This leads to the opening of new voltage gated channels and continuous until the potential level of +20 mV. As suddenly as the sodium channels were opened, they are closed and because of the change of the membrane's polarity, the calcium and more potassium channels are opened, the K^+ ions start to flow out and Ca^{2+} are entering the cell . This persists until the potential levels down to +5 mV, which is called the *plateau* phase. The level of potential is at this state decreasing constantly and as the threshold of -70 mV is crossed, the potassium and calcium channels are closed and we find the cell basically at its initial state, where only a little bit of K^+ ions is leaving the cell. Because of its rapid increase of membrane potential at the first opening of the sodium channels, this kind of AP is called *fast*.

In the ECG, each component represents a step in the heart's excitation and it's connected difference in action potential (as seen in Fig. 2.2). The ECG looks different in each channel according to its possition, but represents always the same component. The P-wave and the first flat phase at the beginning of the AP graph is connected to the depolarisation of atria. QRS complex represents the depolarisation of ventricles, while the PQ interval tells us about the time interval that the pulse needs to get from atria to ventricles. QRS complex itself contains three waves: R-wave is every positive wave in it, Q-wave is the negative wave before the R-wave and S-wave is the negative wave after the R-wave. The T-wave shows the repolarisation of the ventricles. It can be noted, that there is no special feature for the repolarisation of atria. This is because the repolarisation of the atria itself is hidden under the QRS complex where depolarisation of the ventricles is more dominant.

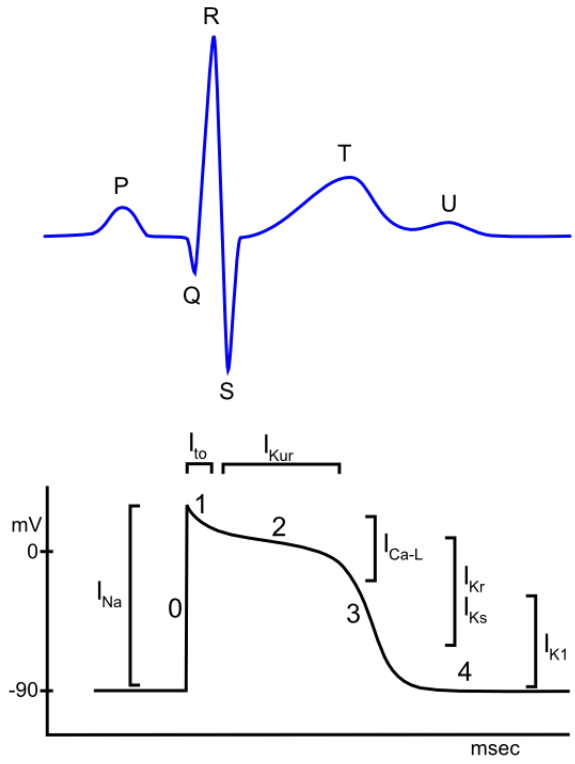

Fig. 2.2: The action potential of cardiac myocytes.

2.2 Genesis of the ECG

In the previous section, there was described the chemical essence of the cardiac activation which is called *depolarisation*. The depolarisation wavefront is transferred across the myocardium. And by delineating this transfer we understand how the electrocardiogram is acquired.

We can look at the propagation of the wavefront as same as is the propagation of signal on the volume conductor. There are two electrodes between which the depolarisation and repolarisation are happening. The positively changed area between these electrodes represents the activated section of the membrane of the cell, and analogous the negatively charged area represents the section of the membrane which is still at the rest. The depolarisation covers the process of signal propagating in the direction from activated section towards non-activated section. We assume that the charge at the rest area and the plateau phase is uniform. Therefore the interface between the activated and section cell can be referred to as a double layer. This double layer is composed of dipoles which together can be identified as *line dipole density source*. The dipole theory is one of the ways how to approach the problem of working heart and will be used in this thesis. The principle of dipole field can be seen in Fig. 2.3.

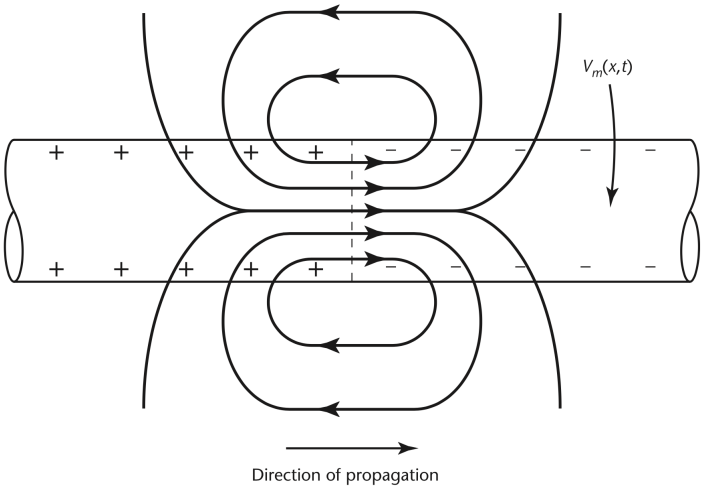

Fig. 2.3: The dipole field due to current flow in a myocardial cell at the advancing front of depolarisation. Vm is the transmembrane potential.

During the depolarisation the dipoles are directed towards the positive electrode (the process is happening in the way of non-activated cells), the signal produced by the activation front will be positive depending on the measuring electrode, type of lead system (uni/bi-polar) and the location. On the other hand, during repolarisation the situation is completely opposite. The repolarisation wave is the process of

membrane getting restoring from the activated phase to the resting. *Vm* is basically negative at the regions of the membrane, where the repolarisation is complete and the membrane is at the rest. Conversely, the regions where the membrane is still at the plateau phase and the repolarisation has not yet begun will be represented by negative *Vm*.

The whole process of electrical activation (EA) of the heart can be described by the progression of the double layer. The EA starts in the sinoatrial node and transfers thought the heart in the direction from endocardium to epicardium and from the apex to the base. The next station of the EA's route is the atrioventricular node (AV node). The propagation through this node is quite slow and cause the pause between the contraction of the atriums and ventricles. This pause is used by ventricles to fill so the blood is not pumped from atria and the ventricles against each other and if it was not present, the heart would not be able to work as a pump. After the AV node the EA continuous with the specialized conduction system that includes the bundle of His, Tawara's bundle branches along with the Purkinje fibers through the inner walls of the ventricles. The result dipole at this moment points to the right and therefore the signal will appear negative. The left ventriculus is thicker than the right one and because of that the depolarisation takes longer. This is the reason why the resultant vector is at the moment pointing leftward. The signal vanishes with reaching the apex of the heart, which id the last to depolarise. Paradoxically, even though the epicardium is the last do depolarise it is also the first to repolarise, because of it's short duration time of the action potential. The repolarisation itself copies the depolarisatioin's route but in the opposite way and heads from the epicardium to the endocardium. In comparison with depolarisation, the repolarisation's signal has smaller amplitude because of it's diffuse character and the whole process lasts longer.

The net dipole of the heart (in Fig. 2.4 indicated by the arrow) as it progresses through one cardiac cycle, beginning with firing of the sinoatrial node (SAN) and finishing with the complete repolarisation of the ventricular walls. Each heart shows the charge separation inside the myocardium, along with a corresponding Einthoven's triangle diagram below it, which displays how the net dipole is defected by each of the bipolar limb leads. Notice the change in direction and magnitude of the dipole during one complete cardiac cycle. The fuse of all of these signal components will result in the elecrocardiogram. [3]

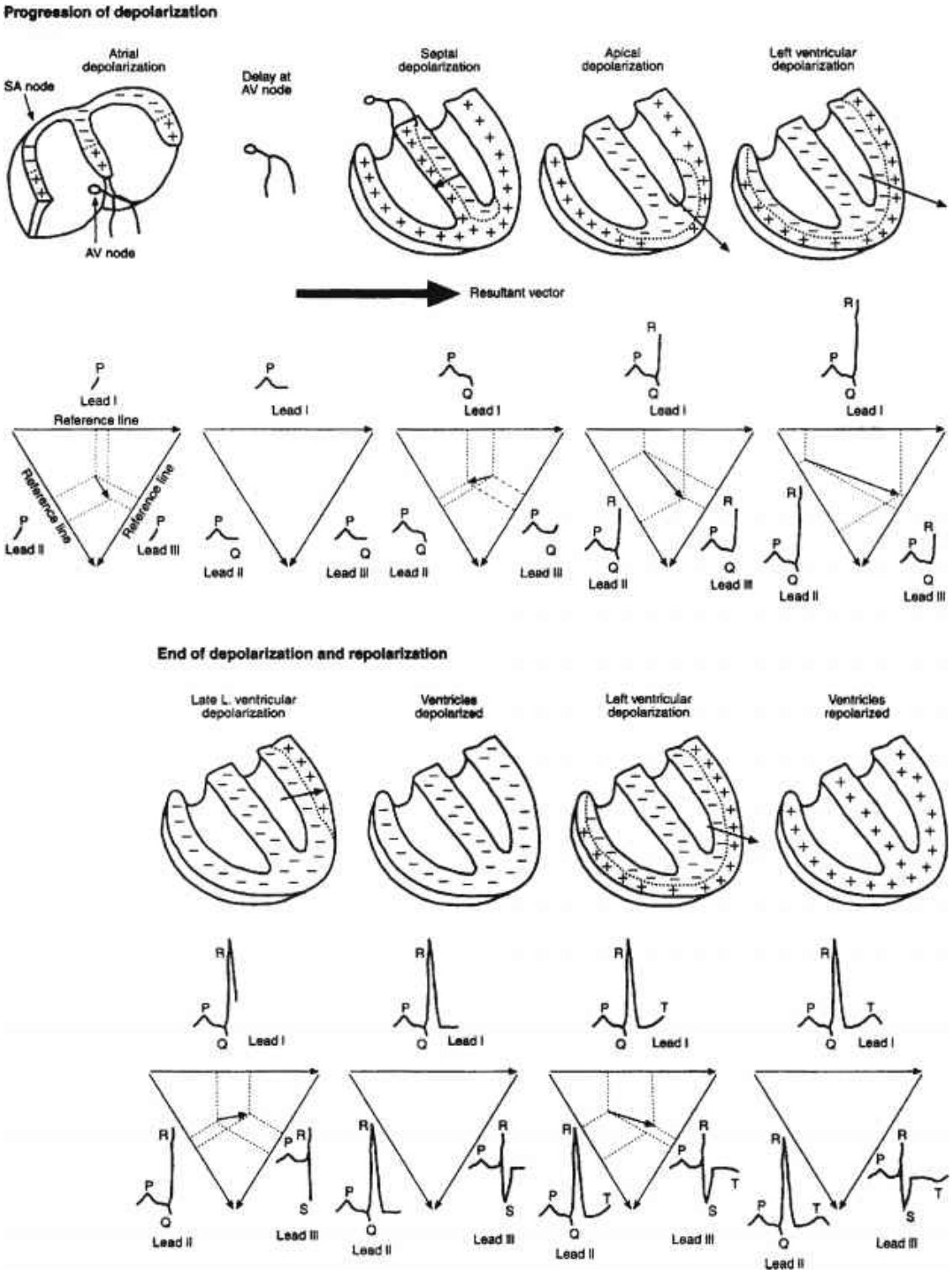

Fig. 2.4: The net dipole through the heart cycle. AV, atrioventricular. Modified from L. R. Johnson (ed.), Essential Medical Physiology, 3rd Ed., 2003.

2.3 ECG and the lead systems

As explained before, the heart works as a volume conductor, can be looked at as a dipole density source and most importantly for scientists - it produces an electrical signal. This signal registers potential differences caused the cardiac excitation and can be monitored non-invasively through the patient's skin . Naturally, there has been developed the need for recording those changes and successively followed by the research.

The history of recording the ECG goes back to the 19th century. Then, the instruments sensitive enough to detect the small current from heart were developed. This progress made it possible for Willem Einthoven, a Dutch physiologist, to first use the term *electrocardiogram*. The year 1903 marks the history of ECG with Einthoven recording the first ECG in a clinically applicable fashion with the string galvanometer.

The leads system used is used until nowadays. The leads were named and still are called **I, II and III** and the electrodes are placed on left wrist, right wrist and left ankle. The arrangement of them creates a system called *Einthoven's triangle* (Fig. 2.5). The potential measured on the right leg is used as a reference potential. The heart lies at the centre of that equilateral triangle. At present we know one other arrangement for those three leads and it consists of using left and right shoulder instead the wrists and lower torso instead of the left ankle. This setting is usually used when eliminating of signal disturbances is needed or for long time Holter recordings. [4]

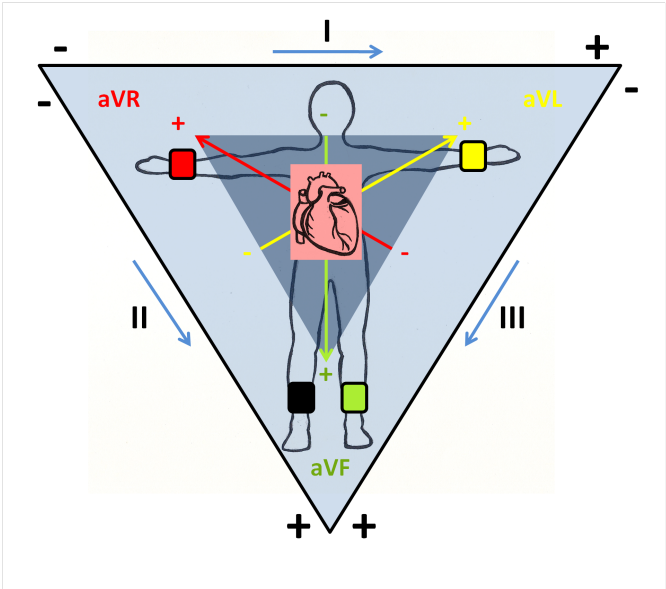

Fig. 2.5: Einthoven's triangle.

The first person who improved the Einthoven's system significantly was Frank Wilson. The idea was including remote reference to the bipolar leads system to create unipolar potentials. With respect to the fact that the volume conductor in question is the size of a human's body that meant connection a 5 kΩ resistor to each terminal of the limb leads. The resulting common point is referred to as a *central terminal*. What the central terminal does is tat it approximates the signal in the infinity. Central terminal is also not independent on the three limb leads, it is, more or less, the average of the three. According to the Kirchhoff's law we know that the total current entering the central terminal of the circuit must add to the zero. Practically it describes the equation 2.1:

$$I_R + I_L + I_F = \frac{\Phi_{CT} - \Phi_R}{5000} + \frac{\Phi_{CT} - \Phi_L}{5000} + \frac{\Phi_{CT} - \Phi_F}{5000} = 0, \tag{2.1}$$

where I_R, I_L and I_F refer to the current components and Φ_{CT}, Φ_R, Φ_L and Φ_F refer to the potentials respectively at the central terminal, right wrist, left wrist and left ankle.

The assumption of the central terminal being the average of the three limb leads leads to the equation 2.2:

$$\Phi_{CT} = \frac{\Phi_R + \Phi_L + \Phi_F}{3} \tag{2.2}$$

The improvement in the form of adding the central terminal is very useful from the reproducibility's point of view. In the clinical cardiology this facility is vital. With the higher resistance, nowadays allowed by the high-input impedance of the ECG amplifiers, would increase the CMRR (Common Mode Rejection Ration) and lessen the artifices at the skin-electrode transition.

Goldberger's augmented leads is the next system that improves the Einthoven's limb leads system. Here, there are three additional limb leads aV_R, aV_L and aV_F. The augmentation of new leads is completed with omitting the Wilson's central terminal. From the equation 2.3 we can see, that the potential at the augmented leads is at least by 50 % larger than the signal with Wilson's central terminal as the reference. In this particular setup, one of these leads is used as a different electrode while the other two together become an indifferent electrode.

$$V_{aV_F} = \Phi_F - \Phi_{CT/aV_F} = \Phi_F - \frac{\Phi_L + \Phi_R}{2} = \frac{2\Phi_F - \Phi_L - \Phi_R}{2} \tag{2.3}$$

The system used in these days by far the most is the 12-lead system of electrodes. This system consists of 3 Einthoven's bipolar limb leads, 3 Goldberger's unipolar augmented leads and 6 unipolar precordial leads (Fig. 2.6). Those 6 precordial leads, which are called V_1 - V_6 are recorded from the left part of the chest. The 6 electrodes creates a semicircle which takes place between 4th and 6th intercostal space, mostly to the left of the sternum. For working in unipolar mode, one of

the precordial leads is used as a different electrode and the three limb leads are connected to become an indifferent electrode. With respect to the precordial leads' characteristics, with choice of any 2 of them the information contained in the gained signal is completely the same as the the amount of information from the residual 4 of them.

Considering the single fixed-location dipole source model, the leads chosen for providing the information needed need to construct 3 components of this model. 2 of the limb leads are reflecting the frontal plane components and one of the precordial leads represents the anterior-posterior component. This setup would indicate the redundancy of the rest of the leads. The model would contain 3 independent and 9 redundant leads. Realistically, there is a need to take into consideration the fact, that the heart involves also non-dipole components, which are quite significant. These components are present mostly at the precordial leads' area. The result of this arrangement is the number of 8 independent leads along side with 4 redundant. The distributed character of cardiac sources is important especially in the pattern recognition.

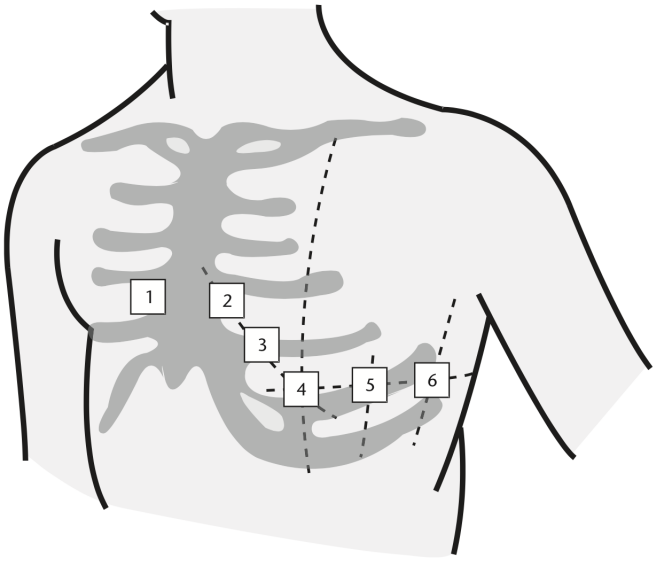

Fig. 2.6: The six standard chest leads.

3 MECHANO-ELECTRIC COUPLING

Mechano-electric coupling (MEC, Fig. 3.1) is a mechanism connecting hemodynamic variables with the heart's electrical activity as the heart is in fact electrically controlled pump. It occurs within the organ itself as an essential for beat-by-beat adaptation. Cardia pacemaker tissue responds to acute changes in mechanical load on a beat-to-beat basis. Electromachanical dyssynchrony can result in various arrhytmias and heart failure. Arrhytmias depend not only on cellular dynamics but also on intercellular coupling, AP propagation and 3-dimentional myocardial structure. If the heart in question in activated dyssynchronously, there regions activates early and late. The early activated regions shorten agains lower than normal loads. The late activated regions are stretched during systole because of the affects of early activated contractions. Normal ventriculas activation is relatively synchronous and causes normal myocardial contraction during the systole, which is the requirement for a proper ejection of blood from the heart. For human heart, the time for completing the ventricle activation is 62-80 ms. This number corresponds to the QRS duration of 70-80 ms. The duration of activation process is the indicative of synchronously activated ventricles. When the duration is longer, it is usually associated with dyssynchronous activation (e.g. left bundle branch block). Epicardial ventricular pacing significantly prolongs QRS duration and has been shown to induce differences in regional workload. Assysnchronous activation during ventricular pacing leads to opposite regions of the ventricles being activated too early or too late, both electrically and mechanically. [6]

Heart muscle adapts to acutely altered mechanical load by a rapid increase of contractile force. The local ventricular repolarisation appears to be synchronized with the pressure dynamics, when the left ventricular load is varied. In isolated rabbit heart, when artificial transient increases in intraventricular volume it causes repolarisation during early systole, depolarisation during ventricular relaxation and with no such effect when applied during an intermediate level of repolarisation. [7]

3.1 MEC in isolated rabbit heart

The ability of the SAN to respond rapidly to the heart's hemodynamics state is the clearest example of the physiological relevance of MEC in cardiac auto-regulation. The increase in the stimulation frequency initiates the increase in the diastolic depolarisation and reduction in AP amplitude. This is represented by a decrease of absolute values of maximum diastolic and systolic potentials. The increase in right atrial BP causes the reduction in the response to vagal stimulation and heart rate acceleration, too. In the beating heart, stretch-induced changes in SAN function

are thought to vary with timing during the cardiac cycle. During acute right atrial dilatation by balloon inflation in isolated rabbit hearts, a global decrease of conduction velocity with stretch has been observed. With volume or pressure overload are associated ventricular tachycardias. The effect of stretch timing in relation to ventricular Vm has been investigated in isolated rabbit heart, which demonstrated that intra-ventricular balloon inflation in diastole causes transient depolarisation, while during the AP plateau it causes repolarisation. This is apparent from isolated rabbit heart studies demonstrating that an increase in intra-ventricular volume results in nonuniform stretch, which is associated with heterogeneity of depolarisation. [30]

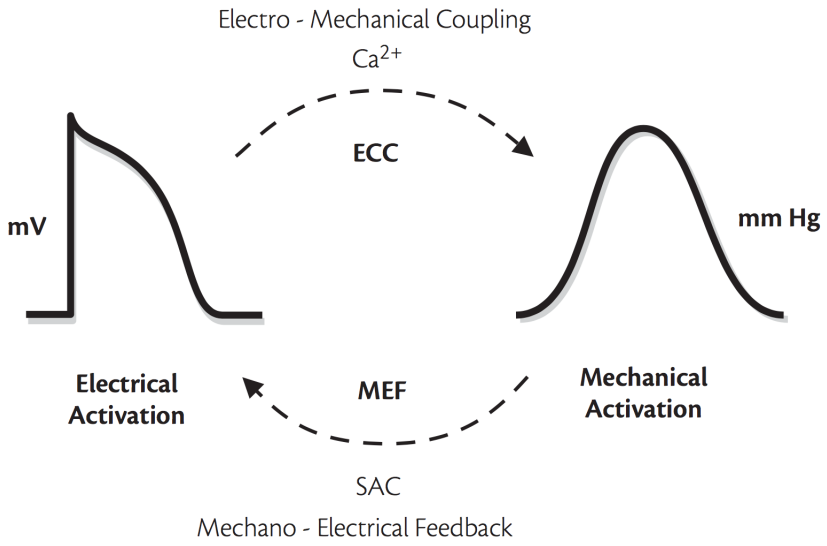

Fig. 3.1: Mechano-electric coupling scheme.

4 SIGNAL AVERAGED ECG

4.1 Basic concepts and features

Signal averaging is widely used technique for the signal analysis. From the historic perspective, it was firstly used in neurological sciences for the denoising the signal. Then, signal averaging has been used for the differentiating of the maternal ECG from the fetus. Another example in the ECG area can be provided with extracting the exercise recording from the movement artifact. The diference between signal averaged ECG (SAECG) and the classic surface ECG lies int he fact, that surface ECG does not provide the information about the electrical activity of the special conductivity system. The catalyst of the method's development was also the lack of understanding of impulse generation in the human heart. The first attempt to use signal averaging was analysing non-invasively (from surface ECG) a His bundle electrogram. Soon after, the attention was concentrated on describing the late potentials, when it was noted, that there was an activation that persisted beyond the QRS complex present. Through the years there was established, that late potentials are the marks of scarred myocardium, therefore the indication of previous heart attack and became essential in reducing the incidence if sudden cardiac death. [5]

Basically, signal averaging as a technique is based on cumulative techniques. There is an assumption of the useful component of the signal is always the same whether the noise components is variating through all the cumulating signals. And therefore, with gradual adding parts to the averaging (cumulation), the noise component will have the tendency to disappear. The purpose of the signal averaging is to improve signal-to-noise ratio (SNR) because, for example, in human ECG signal, temporal and spectral features that identify patients with ventricular tachycardia are masked by the noise with the level of 8 - 10 μV. In human signals, this noise is primarily generated by skeletal muscle activity. There are two commonly known choices of techniques of denoising for using signal averaging - temporal and spacial.

The temporal technique has several requirements to follow if signal is supposed to be analysed with it. Firstly, the signal needs to be repetitive and time invariable. In case there are time varying signals, or parts of them, present in the analysis data, they are excluded from the further analysis. Including those signals would devalue the outcome of the study greatly. [8]

Secondly, the next necessity of using signal averaging is time specificity in the meaning of time locking to the point we can surely address, e.g. the R wave in the QRS complex. If the time locked point are not available, we can realize the analysis using shifting the signal along with observing the changing reference jitter, which can be got by using cross-correlation. Then, we can choose the setting of shifting

signals according to the best correlation.

The third requirement is for the signal analysed and the noise included to be independent (not correlated) and must remain that during averaging.

The noise id additive and is generated by random process with the median of zero. The researcher must know whether it will be possible to accomplish all these conditions at the beginning of the study. The denoising techniques, in this form, are able to reduce the level of noice up to the 1 μV. [9] [10] [11]

4.2 Methods of recording and analysis

The signal averaging is the most generally common technique used to level up the SNR and for analysing high frequency signal components such as *late potentials*. As was mentioned earlier, the signal which is analysed should be repetitive with random noise, the repetitive sequences should be detected and time aligned. However, there are requirements towards the signal which can be fulfilled yet in the recording of the signal. During acquisition, we should be ensured that the signal will be suitable for SAECG analysis. [12]

When choosing the leads system, there is usually preferred bipolar orthogonal leads system over the corrected leads. There exist a possibility of causing the network to be resistor weighting and impedance imbalances would be created. Based on this, the 50/60 Hz interference would be shown and it's intended to avoid this kind of effect. Nowadays, there are many commercial systems. Some of them are specifically prepared for the SAECG recording, others are derived from the classic standard 12-lead system ECG.

All systems designed to record signals for SAECG analysis should have a high quality low rise preamplifier. The gain of these preamplifiers depends upon the dynamic range of the system. The size of the frequency response (output/inout ratio of an amplifier) can be responsible for the distortion of the SAECG and the degradation of the analysis (e.g. late potentials).

The material of electrodes is not the centre of many studies. Many years of practical usage revealed that high quality *Ag/AgCl* electrodes are best for the job. There is one major matter of fact that researches should keep in mind and that is to provide good conditions for the skin/electrode interface. Imperfections in this area lead to the baseline wander and other increases of noise level. The system's ability to eliminate the electrically coupled 50/60 Hz interference is described by the CMRR parameter. [13]

The A/D converter converts the recorded continuous-time analog signal to the sampled discrete-time one. The realisation is done with the respect to the Nyquist-

Shannon sampling theorem. The sampling frequency must be at least twice the size of the highest frequency of interest. Another important attribute of the A/D converter is it's resolution. Usually, the 12 or 16 bit cards are used. The usage of 12 bit card means, that the volts range, e.g. $\pm$ 1 volt, will be divided into 2^{12} levels, which means there will be 0.000488 volts/A/D resolution step.

5 HIGH FREQUENCY ECG AND QRS ANALYSIS

As was stated before, SAECG is used to help analysis of high frequencies of the ECG signal (HF-ECG), e.g for setting late potentials or high frequency QRS complexes (HF-QRS). There are many studies about how is the HF-QRS related to the physiology and pathophysiology of the heart. The example of HF-QRS compared to the normal frequency QRS is in Fig. 5.1

The relation to conduction velocity and fragmentation of the depolarisation wave in the myocardium was stated. The study of canine ECG signals (2 groups - with and without myocardial infarct) that showed that decreasing of the HF-QRS correlated linearly with the local conduction delay. [11]

Other study stands with the opinion that HF-QRS reflects the morphological shape of the original signal. In the study, poor correlation between HF-QRS, which was presented as RMS voltage values of the depolarisation, and signal amplitude was determined. On the other hand, the correlation was high with the first and second derivative of the signal, which means with it's velocity and acceleration.

Also, there is presumed a high connection with the nervous system of the subject. [8]

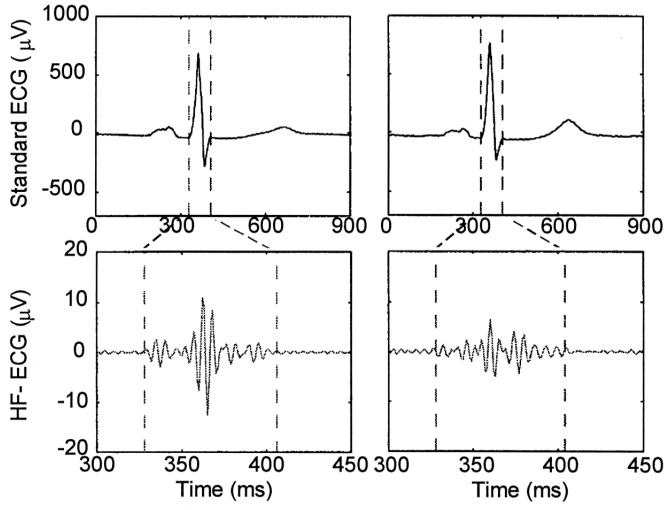

Fig. 5.1: Example of comparison of normal ECG QRS vs. HF-QRS. [8]

The analysis of HF-ECG and HF-QRS contains a list of steps which of some were mentioned before.

5.1 Acquisition

For HF analysis, the signal must be acquired in the best resolution possible and suitable, according to the Nyquist theorem the sampling frequency needs to be at least twice as high as is the highes analysed frequency. In these days, the sampling frequency is not below 1 kHz, work with higher sampling frequency provides more information. Amplitude resolution reaches at least 1 μV. [14]

5.2 Noise reduction

In the HF-ECG and HF-QRS the level of noise in absolute values is significantly lower compared to the normal ECG. Where at classic ECG signal, the noise is in the units of m V, in the HF variant of the signal it is in the units of μV. In ECG measured from human's skin, the source of noise is usually the skeletal muscle. It can be prevented by moving the electrodes to less distant points.

The lowering the noise level can also be interpreted as gaining the SNR. For gaining the SNR is used signal averaging. For this method is important to have enough complexes for the results of averaging to be acceptable.

The changes in the ECG can by examined dynamically. For this case it is useful to use exponentially (recursively) updated beat average, because using standard averaging can be lengthy and is not optimal.

There is need for reference point to align averaged signals properly. Therefore, when using cross-correlation the setup allows to get the best shifting position. Two signals are usually averaged when the correlation coefficient is more than 0.97. There are two most used conditions to stop averaging [18] [19]:

- when the appropriate noise level is reached
- when there is enough acceptable beats for averaging.

5.3 Quantification

Following parameters are the examples of possibilities what to analyse and quantify from the SAECG, or HF-ECG.

QRSd

Filtered QRS complex duration depends highly on the the cutoff frequency. In comparison between normal healthy subjects and subjects with ventricular tachycardia, the QRSd was lengthen with the VT patients. When studying the scale of 10 - 100 Hz, it has been showed that between 10 and 15 Hz, there was a constant increase in

the QRSd. The range of 15 - 25 Hz was characteristic with it's plateau phase and with 40 - 100 Hz frequencies, there was slight constant decrease.

RMS40

Root mean square of the voltage in the last 40 ms of the QRS complex signal is largely exponentially decreasing with the increasing of the high-pass cutoff frequency. The RMS40 was found higher at the normal healthy patients group over those with ventricular tachycardia.

For the quantification of the HF-QRS there have been developed several parameters that can be tracking alongside the ECG analysis.

RMS

Root mean square voltage values are computed during the whole duration of the QRS complex according to the equation 5.1.

$$RMS = \sqrt{\sum_{i=1}^{n} A_i^2/n}, \tag{5.1}$$

where n is a number of measurements and A_i ($i = 1,\ldots,n$) are the measured amplitudes.

For this feature, the exact positions of QRS onset and offset are crutial.

RAZ

RAZ - reduced amplitude zones - are the values that come from morphological measure. It is basically the interval between 2 neighbouring local maxima or minima, which must be at theirs absolute values higher than three preceding and three following envelope points. There are three types of RAZ: 1) Abboud RAZ, 2) Abboud Percent RAZ and 3) NASA RAZ from which can be stated the RAZ score.

Spatial, temporal and individual variation

The amplitude of HF-QRS deffires among all of the 12 leads. The highest amplitudes are observed at the anterior-posterior oriented leads between V_2 and V_4 followed by the interior-psuperior leads II, a_F and III. The smallest amplitudes appear in the left-right a_L, I, $-a_R$, V_1, V_5 and V_6. The explanation of the low amplitudes in the transversal plane could be that leads V_1 and V_6 are the ones most far away from the left ventriculus and therefore the signal is so week. The actual correlation between HF-QRS and QRS amplitudes in the original signal is low.

Variation of the HF-QRS is observed among all of the 12 leads. HF-QRS is again represented as RMS values. Spatial variation speaks about the lead specificity and it's amplitude is the highest at the V_2, V_4, lead II, lead aV_F, lead III. The The sum of the RMS values for the 12 leads is between 20 and 75 μV for human experiments. Individual variation is not very correlated between more subject and therefore it was accepted that it is a useful feature for monitoring of one patient over the time and is used for setting normal limits above population. The variation is more sensitive in diagnostics of acute ischemia than ST segment deviation. Temporal variation is computed for assessing dynamic changes. Finding out the variance of the HF-QRS is also desirable for specify the noise level. It can be defined as a RMS during 100 ms, starting 100 ms after QRS offset. When the noise level was > 0.75 μV, the lead data are excluded from the analysis.

The HF-QRS can be monitored in various non-physiologic situation, which of one is stressed induced ischemia. RMS voltages during exercise are increasing in the group of healthy normal patients. In comparison with the group of patients with ischemic heart disease, the amplitudes of voltages are higher in the healthy group during and even after excercise. The the morphological point of view, the analysis of resting morphology (RAZ counts) and the analysis of the dynamic changes in amplitudes (RAZ voltages) can be provided. HF-QRS was highly sensitive (94 %) and specific (83 %) for the detection of reversible perfusion defects. Compared to the conventional ST-segment analysis, the HF-QRS is significantly more sensitive (by 18 %).

Conduction abnormalities are quite common to be noticed after the myocardial infarct. The HF-QRS is reduced, when there is slow conduction velocity. Experimentally, it can be shown by using sodium blockers. When applied to left anterior descending coronary and compared with the rest of the heart, the amplitudes are lower in the affected area. HF-QRS is therefore a potent marker of damaged local conduction.

PRACTICAL APPLICATION

6 EXPERIMENTAL DATA

6.1 Perfusion system

The model of isolated rabbit heart provides the measurement of various indices and permitting detailed analysis. The systemic interferences as e.g. sympathetic and vagal stimulation or alternations insystemic and pulmonary vascular resistance and left and right ventricular loading.

For the acquisition of the data is used the combined setup of Langendorff and Neely perfusion system. The Neely system is a follower of previously founded Langendorff.

The model of isolated animal, mammalian, heart was found and described by Langendorff (1895). It is a wide-ranged system permitting the analysis of hearts from e.g. guinea-pigs, mice, rabbits or rats. In this case, only the heart's aorta is cannulated (when cut just below the point of its division). The system can work in two modes - constant pressure or constant volume and is built on the principle of *retrograde direction pumping*. The retrograde direction means that the fluids are pushed from the aorta through the aortic valves to the heart's coronary arteries. The closure of the aortic valves corresponds to the diastole, the phase of a heartbeat when the heart relaxes and the chambers are allowed to be re-filled with blood. Because of this sequence of actions, the ventricles are not filled at all and therefore no pressure-volume work is done. It is the reason why Langendorff provides energetically less demanding isovolumetric contractions. There are many parameters, which can be tracked by this model, e.g. contractile force, cardiac rhythm or coronary Volume (provided by countdrop).

Nevertheless, the perfusion system used in this case was first described by Neely in 1967 and it simulates the model of working heart. It represent the physiological character of the heart more appropriately and is more suitable for the mechano-electric coupling analysis.

The working, fluid-ejected heart performs pressure-volume work, which causes less energetically demanding isovolumetric contractions. The heart is perfused via the left atrium, mitral valve and eject fluid through the left ventricle into the aorta. During the systole left ventriculus ejects the buffer back to the reservoir and the heart's own coronaries are perfused.There is a possibility to measure the cardiac output continuously as the sum of aortic and coronary flow.

Prior to the first experiment of the day the working heart apparatus should be flushed with purified water. The cannulated heart is transferred to the apparatus. The aortic connector for the cannula should be gently dripping with perfusate and the cannula approximated to the connector at an oblique angle to avoid air emboli

at the time of heart attachment to the apparatus. To ensure unimpeded drainage of coronary venous perfusate the pulmonary artery should be incised. This is advisable as the close proximity of the pulmonary artery to the aorta and the con- nective tissue surrounding both vessels result in relatively frequent, inadvertent liga- tion or at least partial obstruction of the pulmonary artery. The incision also facilitates later cannulation of the pulmonary artery if arterial-venous differences in perfusate oxygen content are to be measured. The atrial cannula should be driping with perfusate when being inserted so that any air present in the left atrium or ventricle is removed. The cannula is then tied into the left atrial wall by securing the left atrial tissue surrounding the orifice above the flange at the distal end of the cannula with a suture. After instrumentation of the heart is completed (usually within 5 min after initiation of Langendorff perfusion, the heart is left for 15-20 min to equilibrate under retrograde perfusion preferably under 100 mmHg constant perfusion pressure. It should be noted that there is no flow to the atrial cannula at this stage. After enabling flow through the aortic cannula, flow in the aorta should be reversed as the heart begins ejecting perfusate in an antegrade fashion and the aortic perfusion pressure becomes afterload. [15].

Afterload, preload, left ventricular pressure (LVP), atrial flow, aortic flow as well as the electrocardiograms are measured continuously.

In the Fig. 6.1, the simplified scheme of the Neely system is displayed.

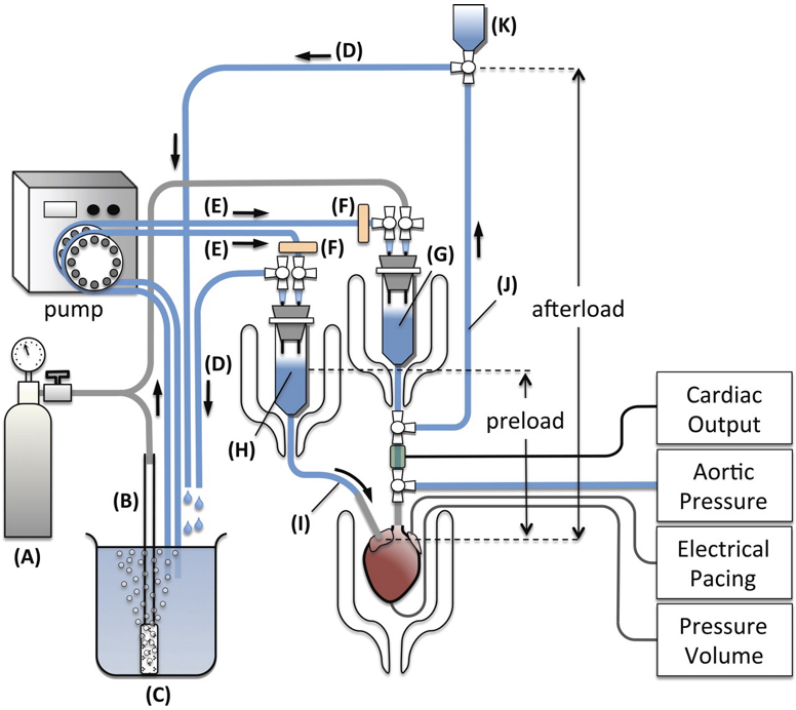

Fig. 6.1: Simplified scheme of a Neely working heart model system.

6.2 Preload and afterload

For understanding the data it is crucial to pay attention to the concepts of preload and afterload.

6.2.1 Preload

Preload describes how much is the myocard flexed before the contraction at the end of diastole. It also refers to the amount of volume in the ventricle at the end of this phase. The greater the stretch, the greater the force of contraction. An increase in the stretching of the myocard will cause an increase in the force of contraction, which will increase cardiac output. Preload largely depends on the amount of blood in ventricle. The amount of blood returning to the heart in any period of time must be equal to the amount of blood pumped by the heart in the same period, as there is no place for storage of blood in the heart. Venous return therefore equals cardiac output, whereas preload is only one component of cardiac output. [16] [17]

6.2.2 Afterload

Afterload is the force against which the ventricles must act in order to eject blood, and depends on the arterial blood pressure and vascular tone. Afterload depends on a number of factors, including volume and mass of blood ejected, the size and wall thickness of the ventricles, and the impedance of the vasculature. The most sensitive measure of afterload is systemic vascular resistance for the left ventricle and pulmonary vascular pressure for the right ventricle. Afterload has an inverse relationship to ventricular function. As resistance to ejection increases, the force of contraction decreases. Reducing afterload will increase cardiac output.

6.3 Methods

6.3.1 Preparation

High resolution ECG signals were gained from isolated hearts of New Zealand rabbits. Each experiment was held at one rabbit when the animal was sedated to the general anaesthesia in the form of injection of xylazin, diazepam, heparin and ketamine. When the animal is completely under the influence of the medication, the heart is taken out of its body, it is inserted into the perfusion system and aorta and left atrium are cannulated. In this phase, the perfusion is realised according to the Langendorff by oxygenated (95 % 0_2, 5 % CO_2) Krebs-Henseleit buffer (1.25 mM Ca^{2+}, 37 °C).

6.3.2 Acquisition

The heart is kept in the bath with the buffer, which is a part of the perfusion system, and the signal is gained by non-contact method by using the seven unipolar *Ag-AgCl* electrodes placed on an interior wall of the chamber. Electrodes were uniformly spaced along the semicircle so that electrical activity of the entire left ventriculus was recorded. Also, the standard three bipolar X, Y, Z leads can be derived. The placement of the electrodes can be seen in the Fig. 6.2.

Data were acquired by measuring card with the 16 bit resolution and the sampling frequency of 10 kHz. 16 bit resolution is enough for this kind of data recording as the amplitudes we are after are in the units of μV to mV. [20] [21]

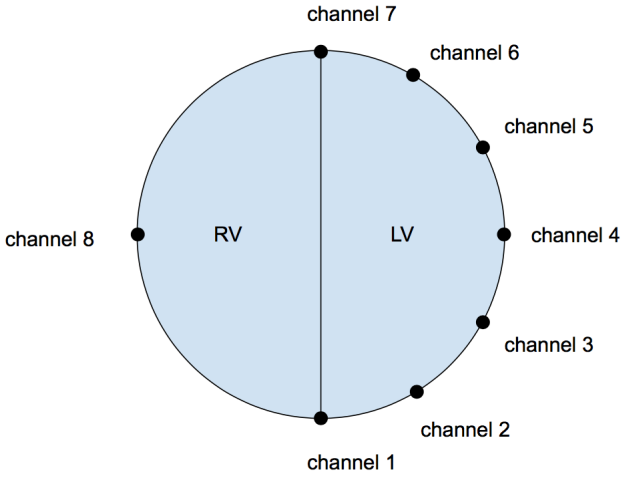

Fig. 6.2: The placement of the electrodes during the experiment (RV - right ventriculus, LV - left ventriculus).

6.4 Experimental protocols

The data analysed in this thesis have been gained from two experiment protocols with labels 2.0 and 3.0. Those were set ahead the start of the data acquisition and the example of the 3.0 version protocol can be seen in the Fig. 6.3.

When the heart is cannulated, the first 15 minutes long part is in Langendorff mode with constant pressure of 80 mmHg. After the stabilisation of its action, the mode is switched to the perfusion according to Neely (preload: 8 cmH_2O; afterload: 60 cmH_2O) following by 15 minutes long stabilisation. The protocol consists of

intervals which differ between each other with its preload, afterload and stimulation frequency being changed.

6.4.1 Protocol 2.0

The protocol 2.0 was performed in the first set of experiments in the year 2016 and is a source of 8 out of 15 analysed experiments. Preload in this protocol switches between the values 8 and 11 cmH_2O which every of those values appears during the experiment twice. During every stable stage of preload the stimulation frequency undergoes the change from 270 to 320 ms and back. This process is completed four-times. Afterload here keeps the value of 60 cmH_2O until the last stage of preload where it switches to 80 cmH_2O and back.

6.4.2 Protocol 3.0

The protocol 3.0 was performed in the second set of experiments in the year 2016 and is a source of 7 out of 15 analysed experiments. It differs from the protocol 2.0 in the number of changes executed, which is lower. In the first stage preload and afterload are stable at the values of 8 and 60 cmH_2O. During this stage the stimulation frequency switches from 320 to 270 ms and back (in one experiment from 350 to 300 ms and back). After, preload rises to 11 cmH_2O followed by afterload, which goes from 60 to 80 cmH_2O. Afterload is also the first one to dip again to 60 cmH_2O and then preload goes back to it's initial 8 cmH_2O.

Altogether, 15 experiments have been used, including 8 pseudo-ECG channels monitoring left ventriculus, left atrial pressure and Volume, aortic pressure, information about the temperature. In the setd of provided data there were included the global positions of R-wave, cycle position, T-wave peak and offset, systolic, diastolic and end-diastolic pressure. The overview of data used for analysis in this thesis is listed in Tab. 6.1. [20] [21] [22] [23] [24]

Because of the condition of several signals from channels 3 and 5 (unremovable high level of noise, disconnection of electrode) it was decided that those channels will be excluded from the analysis in all experiments.

Tab. 6.1: The overview of used data provided for every experiment

Data	Explanation	Unit
eg1 - eg8	ECG signal channels	[mV]
BP_Ao	Blood pressure in aorta	[cmH2O]
BP_LA	Blood pressure in left atrium	[cmH2O]
Flow_Volume	Volume of blood which flows through left atrium per 1 beat	[ml]
Cycle_Pos	Positions of cycle in the experiment progression	[sample]
Pressure_Sys_Val	Values of systolic aortic pressure	[cmH2O]
Pressure_Dia_Val	Values of diastolic aortic pressure	[cmH2O]
Pressure_Dia_End	Values of end-diastolic pressure in left ventricle	[cmH2O]
QRS_onset	Positions of the QRS complex onset	[sample]
R_wave	Global positions of R-wave in the experiment progression	[sample]

6.5 Data used in the analysis

In the following paragraphs the most important data that have been used for the analysis are described more into detail, mostly about how they describe the left ventricle and their importance for understanding the working heart will is explained.

6.5.1 $eg1 - eg8$

These 8 variables contain the data about electric activity of the left ventricle. The positions of electrodes while measuring the left ventricle can be seen in the Fig. 6.2. The unit of these signals is [mV] and we are trying to explain the reactions of those signals according to the hemodynamic (pressure and volume) parameters.

6.5.2 BP_Ao

BP_Ao contains the data about aortic pressure. As the left ventricle ejects blood into the aorta, the aortic pressure increases. The greater the stroke volume, the greater the change in aortic pressure during ejection. The maximal change in aortic pressure during systole (from the time the aortic valve opens until the peak aortic pressure is attained) represents the aortic pulse pressure, which is defined as the systolic pressure minus the diastolic pressure.

6.5.3 *Flow_Volume*

The *Flow_Volume* represents the amount of blood (solution) that is ejected from the left atrium to the left ventricle during one heart beat. It is used as an estimation of the volume which is present in the left ventricle in the moment of heart contraction. The term of estimation is used because it cannot really be stated how much of left atrium volume is left there when ejected to the left ventricle.

6.5.4 *Pressure_Sys_Val*

When the left ventricle ejects blood into the aorta, the aortic pressure rises. The maximal aortic pressure following ejection is termed the systolic pressure.

6.5.5 *Pressure_Dia_Val*

As the left ventricle is relaxing and refilling, the pressure in the aorta falls. The lowest pressure in the aorta, which occurs just before the ventricle ejects blood into the aorta, is termed the diastolic pressure.

6.5.6 *Pressure_Dia_End*

End-diastolic blood pressure is the pressure value at the end of the diastole, which is the period during which the ventricles are filling and relaxing. If ventricular compliance is decreased, the ventricle is stiffer. This results in higher ventricular end-diastolic pressure. If ventricular compliance increases, the end-diastolic pressures may not be greatly elevated.

The experiments performed to acquire the data took place in the laboratory of the experimental cardiology at the Masaryk university in Brno. They were performed in accordance with the guidelines for animal treatment approved by local authorities and conformed to the European union law.

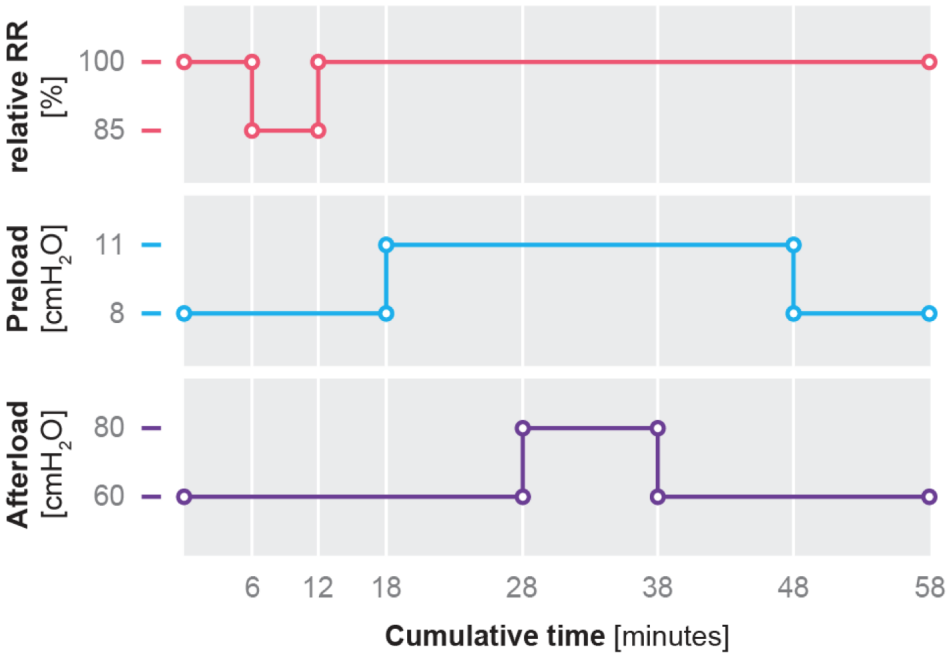

Fig. 6.3: Experimental protocol version 3.0.

7 FREQUENCY BANDS FOR ANALYSIS

The standard for the analysis in different frequency bands of isolated rabbit heart's ECG is mainly based on the same principle as the analysis of the human ECG. The frequency bands for the human ECG analysis have been studied into details. Usual band of frequencies of interest is up to 125 Hz, for children up to 150 Hz. This band consists of most of the important normal ECG features, such as QRS complex. All the information contained in the QRS complex falls between 3 and 40 Hz, when the maximum of energy of the signal lies between 10 and 15 Hz (sometimes 5 - 20 Hz). The band of high frequencies was, also because of historic issues, settled at 150 - 250 Hz. Normalised standardised frequencies create bands: ultra low frequencies (ULF) < 0.003 Hz; very low frequencies (VLF) 0.003 - 0.05 Hz; low frequencies (LF) 0.05 - 0.15 Hz and high frequencies (HF) 0.15 - 0.40 Hz, which means that the total range of analysed data was 0 - 1500 Hz. [25] [26]

It is known that frequency spectrum of the rabbit ECG signal is significantly shifted towards the higher frequencies (Fig. 7.1). The band for the whole QRS information is considered between 13 and 73 Hz, which responds to approximately triple the human ECG QRS band. The same situation is present with the band of common interest. For rabbit signals it is considered to up to 225 Hz, which is also double the human frequency band of common interest.

From these facts can be settled that the bands for high frequency analysis of isolated rabbit hearts should start at at least 300 Hz and will continue towards higher frequencies. The lower border of HF frequency analysed band is set to 300 Hz, because up to this point there are present components of normal ECG. The aim of this thesis is to explore the content of HF section of ECG signal with the connection to the change of hemodynamic parameters. Therefore it was decided, that the start point for the analysis will be five, relatively wide, bands:

- 300 - 500 Hz
- 500 - 700 Hz
- 700 - 1000 Hz
- 1000 - 2000 Hz
- 2000 - 3000 Hz

Later, it will be found out, that the range is over exceeding its necessary width, because the two highest frequency bands consist only from random noise without useful information gained with this processing.

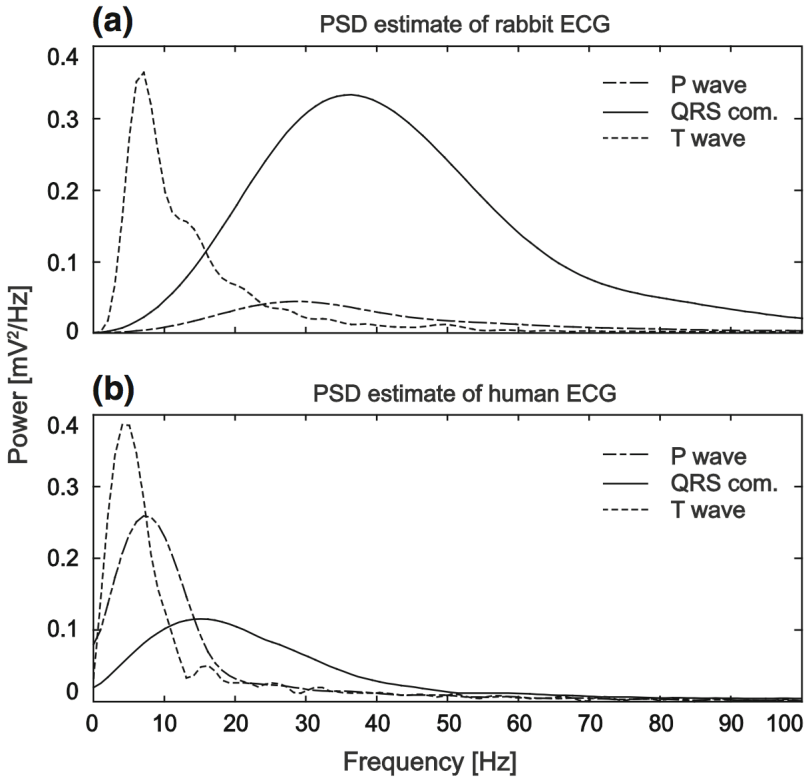

Fig. 7.1: Comparison of power spectral density (PSD) of individual waves between (a) isolated rabbit heart and (b) human ECG signal.

8 DESIGN OF THE ANALYSIS

One of the partial aims of this thesis was to design an appropriate algorithm for the preprocessing of the HF-QRS analysis, preparing the signal and evaluate the parameters chosen for this particular analysis. This algorithm must respect all the information gained with literature review and also the physiological predisposition of isolated heart from rabbit. The design of the algorithm can be seen in Fig. 8.1.

Experimental data enter the analysis in their raw form and during the preprocessing there is no filtering apart from the baseline wander removal. In the clustering part are the sections of signal sorted according to their morphology. After that, it is time for decomposing HF part of the signal's spectre into bands. At the end of the master's thesis analysis, there will be set of bands which are the most convenient for HF-QRS analysis. After signal is decomposed, there come the evaluation by the parameters. At the beginning of the analysis, there stand parameters for standard HF-ECG analysis (late potentials) - duration of the QRS complex, the width of the Hilbert envelope in the respected frequency bands, the maximum of the signal in respected bands in the QRS area, RMS of the same are and the position of the maximum towards the global position of R wave.

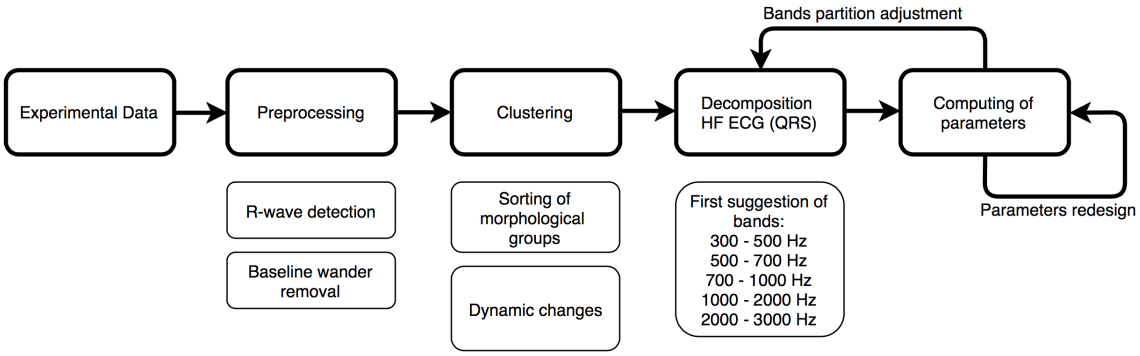

Fig. 8.1: Flowchart of the HF-QRS analysis.

8.1 Preprocessing

The data analysis input contains the outcome of 8 ECG signal channels, aortic pressure channel and left atrium blood volume channel and the analysis is done at each channel respectively.

8.1.1 Baseline wander removal

The first part of preprocessing is levelling up the baseline. As because the human heart is not recorded in its isolated state, a few effects can cause such a thing as baseline wander. There is respiration, body movements or electrode/skin impedance mismatch. All together they can cause an interference usually up to 0.1 Hz and the morphology of the beat could be changed. In isolated heart, neither of those phenomena are present. In spite of this, with visual control of the data was found that there were parts of the signal slightly wandering. Because one of the steps of the analysis includes morphological clustering, the same baseline is much wanted effect. If the wandering was caused by the heart moving, it would have been with the frequency of the heart rate, which is for rabbits circa 240 bpm. This would cause an interference at 3 Hz, which would lead to a wider stop-band than required. Electrode/skin impedance is not very likely to be present as the electrodes are placed around the heart in the wall of liquid chamber. Other sources of the interfering frequencies were probably the movement of the heart itself, the fluid solution passing through the heart or by the movement of the whole perfusion system or other unpredictable situation. [5] [27] [28]

8.1.2 Choice of filter

There has to be a filter which is stable and will cause no damage of the proceeding signal. The Butterworth IIR filter was used with the order defined by MATLAB's `buttord` to 4 and for actual filter designed by function `design`. The magnitude response of the filter can be seen in Fig. 8.2. The final value at -3 dB of designed filter was 0.32 Hz, with which was achieved the expected outcome of levelling up the baseline wander (Fig. 8.3). This step of preprocessing the signal has applied for all the ECG channels and from this point on the analysis continued with the outcomes. [29] [30]

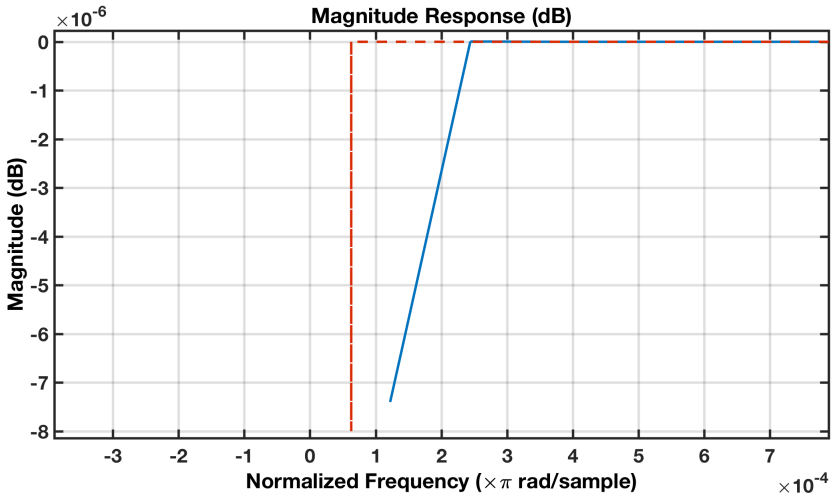

Fig. 8.2: Magnitude response of the high-pass filter.

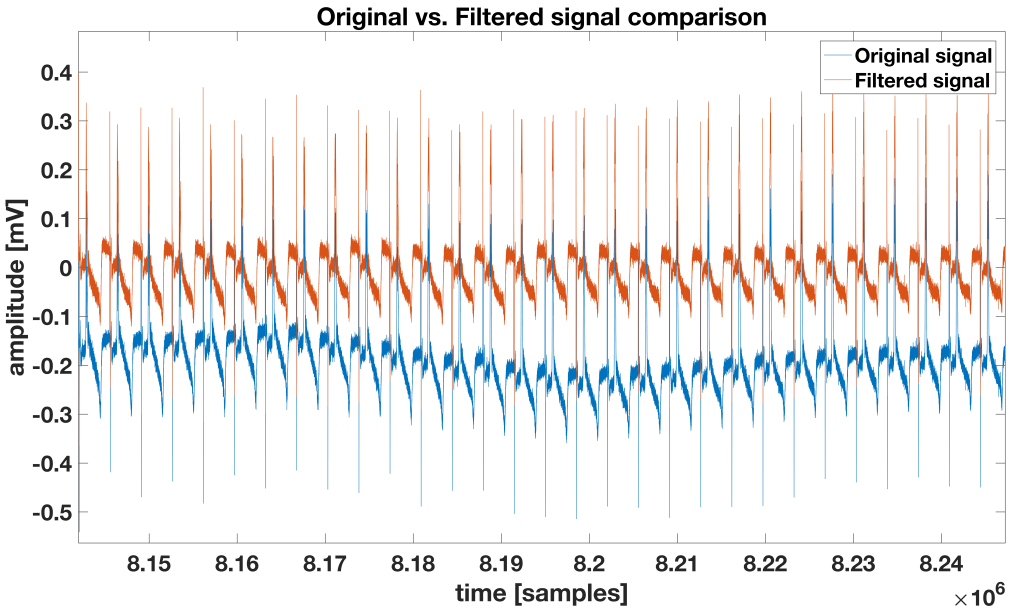

Fig. 8.3: The comparison of original and filtered section of signal.

The next step of the analysis is using the global R-wave positions in the signal to extract the periods of the signal in the vicinity of those points. The length of the period was chosen for 120 ms, as for the normal duration of QRS complex in rabbit heart is 35 ms (with the range of approximately 20 - 70 ms).

8.2 Signal clustering and averaging

Data prepared like previous paragraph described are the input for the sorting and averaging part of the analysis.

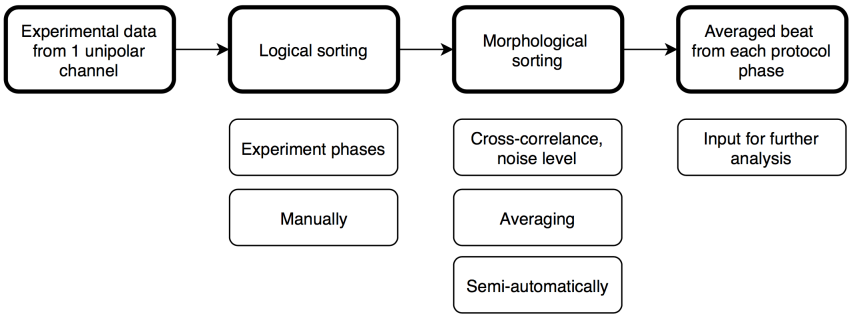

Fig. 8.4: The flowchart of the clustering part of the analysis.

8.2.1 Choice of experiment phase

For the clustering part of the process there is a necessity to have a reference point according to which there will be the aligning provided. In our case, these points are the global R-wave positions that are present for all the parts of experimental measurement. The process of clustering is done channel by channel sorted separately. In the first step, we provide the algorithm with information, what part of the experimental protocol is being analysed. The extracted part of the signal is in the algorithm called `section`. The number of sections included in the experimental measurement is variable according to the length of the experiment and according to the number of changes done with the incoming parameters. The mean number of sections per experiment is 10.47 ± 3.81. The 8 experiments measured under the protocol 2.0 had the mean number of sections 13.12 ± 3.18 and experiments under the protocol 3.0 7.43 ± 1.40. That is the reason why this part is only partly automatic and the start and stop points of each mentioned part need to be specified manually.

8.2.2 Aligning of beats

When the wanted part of the experiment is chosen, the signal enters the sorting clustering function alongside with the global R-wave positions. The process of clustering done with parts of the signal with the length of 1200 samples, which equals to 120 ms, 60 ms on each side from the selected R-wave position. The size of the windows was chosen according to the average width of the QRS complex in rabbit ECG signal and also the stimulation peak was not included.

At the beginning, the first two following R-wave positions are chosen and the signal around them extracted. These two parts (one is set as a template, the second one is unassigned beat) of the signal enter the phase of cross-correlation with the possibility of moving one signal alongside the other one within the range of maximum lag, which was set to 20 ms around the R-wave possition. For this range, the cross-correlation is computed for every position. Out of all possible settings, the one with the highest index of correlation is chosen. If that index is exceeding 0.985, the two analysed parts of the signal are said to be from one morphological group. For this group the information are held about which R-wave positions are included, the signal parts held in a matrix (including the possibly present shift) and newly computed average beat. This average beat is from now on the template used for finding out, whether the unassigned beat belongs to the morphological group or not and is updated with every added signal part.

If the maximum index of correlation is not bigger then 0.985, new morphological group is created. With the increasing number of morphological groups, firstly the unassigned beat is cross-correlated with all the existing ones and only with the negative result with each of them the new group is created. At the end, there is a set of groups of correlated signals. Each group consists of the matrix of parts of signal involved with their positions in the analysed signal and the averaged beat of the whole group. The purpose of this step, to gain higher SNR, has been achieved by averaging 990 ± 533 beats (in protocol 2.0 were, compared to protocol 3.0, shorter phases in-between changing the input parameters which is a reason why standard deviation is so high).

The outcome of aligning from the section of signal from the beginning of the experiment can be seen in Fig. 8.7. The parameters for this particular section were preload 8 cm, afterload 60 cm and stimulation frequency 270 ms and the source is channel 1.

8.2.3 Manual control of outcomes

It is possible to happen, that after the first sorting step, the number of groups will be too high. With visual control, it can be found, that some of the groups evidently belong together. The example of that can be seen in Fig. 8.5, where the algorithm decided to create 2 morphological groups when obviously, the beats belong to one. This could have happened because of one cross-correlation coefficient being not 0.985, but e.g. 0.983. If that is the situation, the groups are once again manually checked, whether they do not share correlation coefficient high enough to be merged. The example of signal being correctly separated into 2 different groups can be seen in Fig. 8.6.

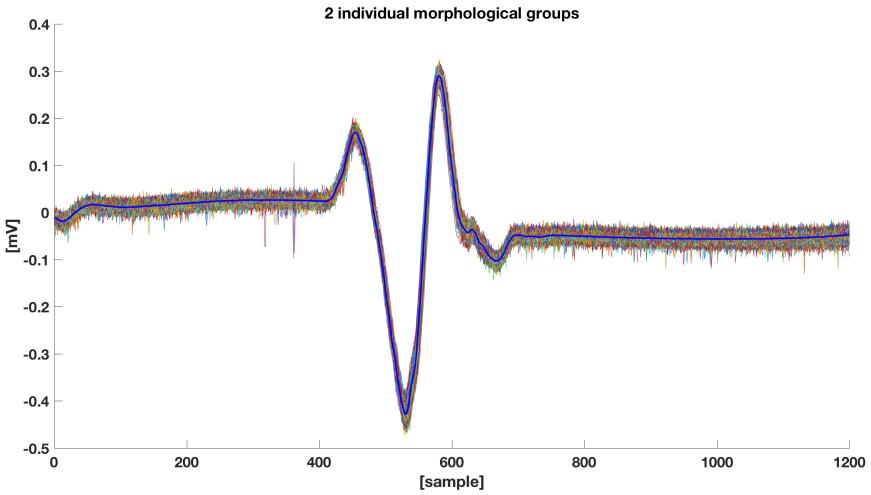

Fig. 8.5: The example of 2 merged morphological groups.

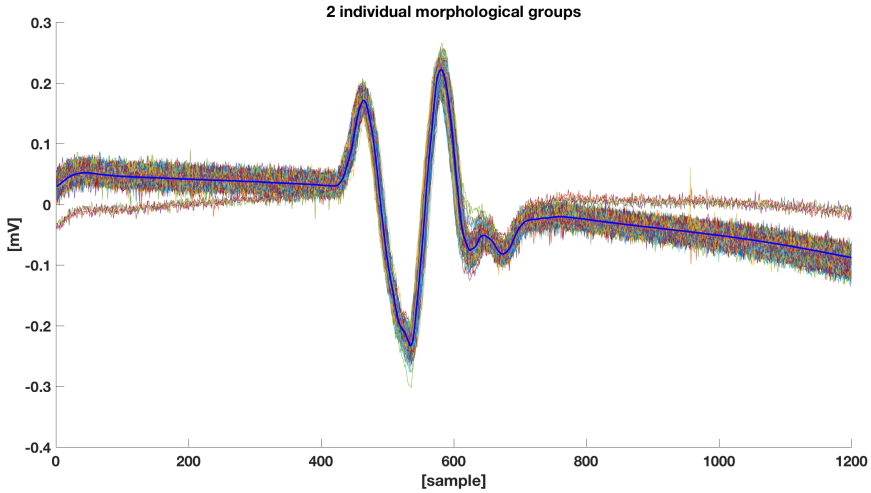

Fig. 8.6: The example of 2 not merged morphological groups.

Every morphological group represents the part of the signal which is stable in its shape and amplitude. In 15 analysed experiments, this stable phase does not include the phase immediately after the change of the parameter (the very beginning or the end of the signal section). The aim of this thesis is to describe the behaviour of the isolated rabbit heart, specifically the HF-QRS part of ECG signal, as a reaction to the change of hemodynamic parameters, aortic systolic pressure and left atrium volume. Therefore, these two parameters need to go through the very similar algorithm. At the end of this piece of program we are presented with the average values of pressure and volume for every section of each protocol. The process of clustering is provided for all 8 ECG channels, aortic systolic pressure and left atrium volume

and it's process is illustrated in the Fig. 8.4 . The functions which are responsible for this part of analysis are `ClusteringFunction` and `SortingBPFlow`.

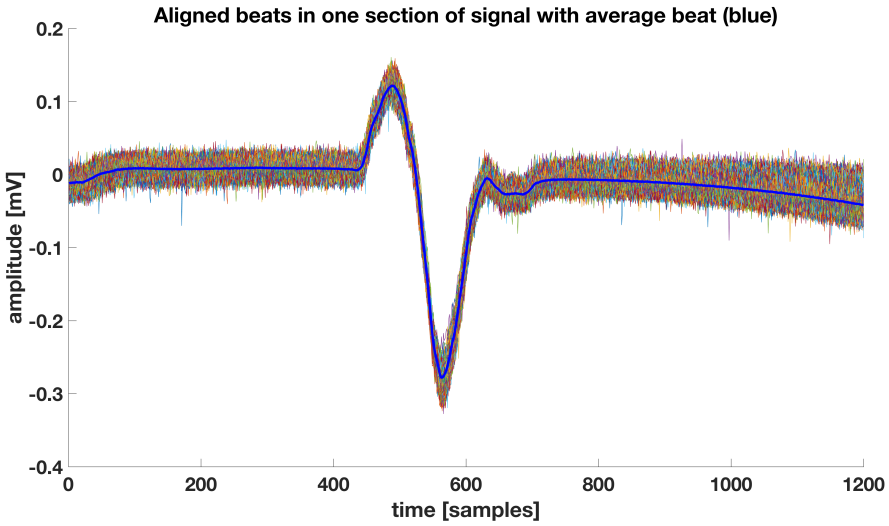

Fig. 8.7: Aligned beats with the resulting average beat.

The outcome of this part of the preprocessing are the structures containing the mentioned information - signal included in respected sections, indexes of positions of beats chosen for the analysis and the averaged beat. The structure is constructed in the style: `signal -> sections of protocol -> leads 1-8`.

8.3 Signal decomposition

Following part of the analysis consists of subjecting the averaged beats to a decomposition into separate frequency bands. As was described earlier in this thesis, the number of bands have been settled to to 5, with the parameters described in the table 8.1.

Serious number of various filters have been tried, starting with the recommended 4th order Butterworthfilter [10], unfortunately, this filter has caused unrepairable damage to the signal in all analysed frequency bands with much significant transition hase. After this unsuccessful attempt have been tried many other filter settings, which included mostly trying filters with gradually increasing filter orders (from order 4 to order 70 with tmean step of 5). The choice process has ended with using FIR filters all stable with orders from 15 to 70 with the effective values at -3 dB exactly the bands' borders. All the filters' settings can be seen in the Tab. 8.1 and the filters' characteristics in the Fig. 8.8, 8.9, 8.10, 8.11 and 8.12.

Tab. 8.1: Characteristics of filters used in signal decomposition

Band no.	**-3 dB frequency [Hz]**	**Order**
1	300-500	70
2	500-700	70
3	700-1000	50
4	1000-2000	15
5	2000-3000	15

For every section in every analysed lead in every experiment have been computed five different filtered signals. The example of them can be seen in the Fig. 8.13. For each of those signals have been computed the Hilbert's envelope with the Hilbert transformation to enter the further analysis. The examples of envelopes can be seen in the Fig. 8.14. All the data are, again, saved in the special structure which enters the next step of analysis.

From the Fig. 8.13 is evident, that the last two bands with the highest frequencies are mostly composed from random noise components. Therefore, into the next step of analysis will continue only data from the first 3 bands with the range of 300-1000 Hz.

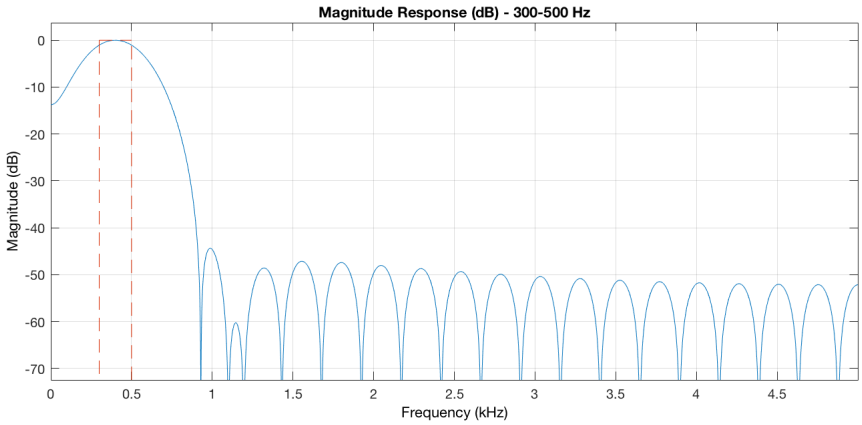

Fig. 8.8: Characteristics of a band-pass filter 300-500 Hz.

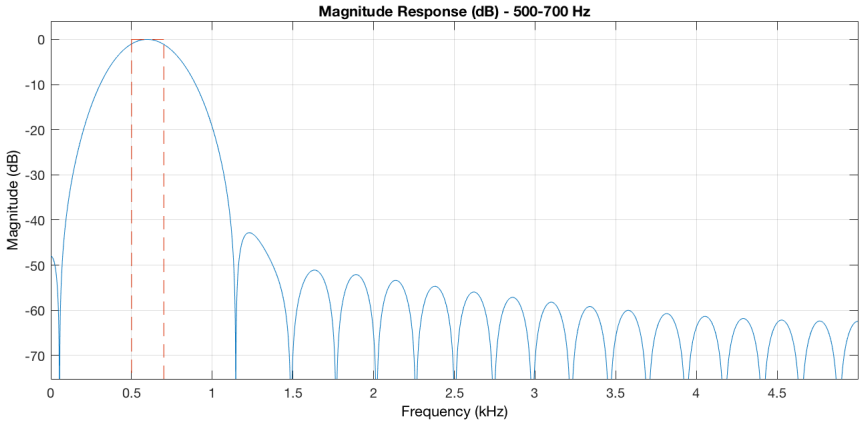

Fig. 8.9: Characteristics of a band-pass filter 500-700 Hz.

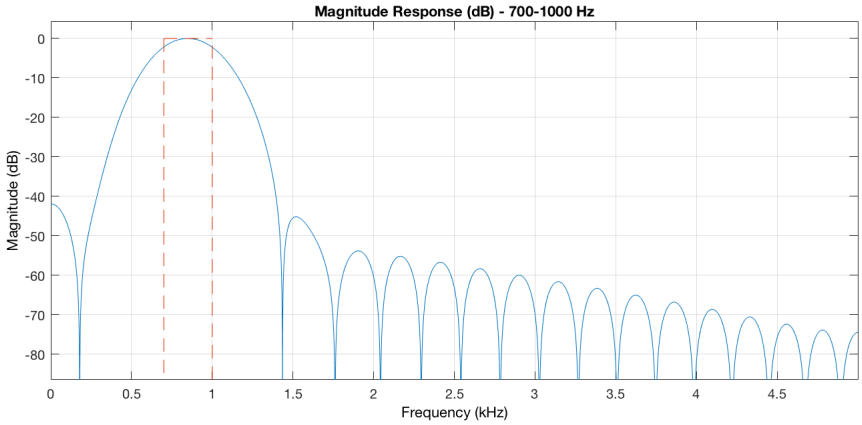

Fig. 8.10: Characteristics of a band-pass filter 700-1000 Hz.

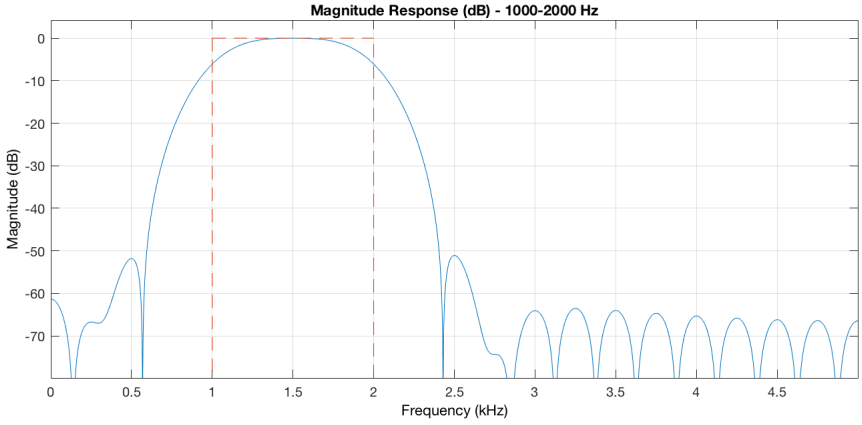

Fig. 8.11: Characteristics of a band-pass filter 1000-2000 Hz.

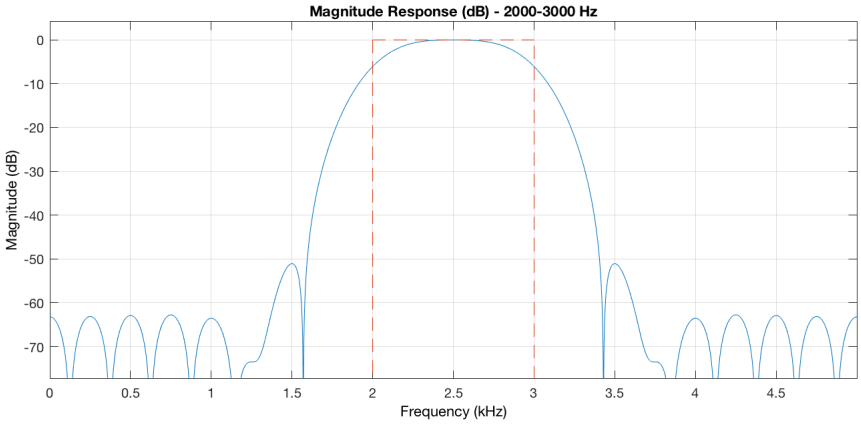

Fig. 8.12: Characteristics of a band-pass filter 2000-3000 Hz.

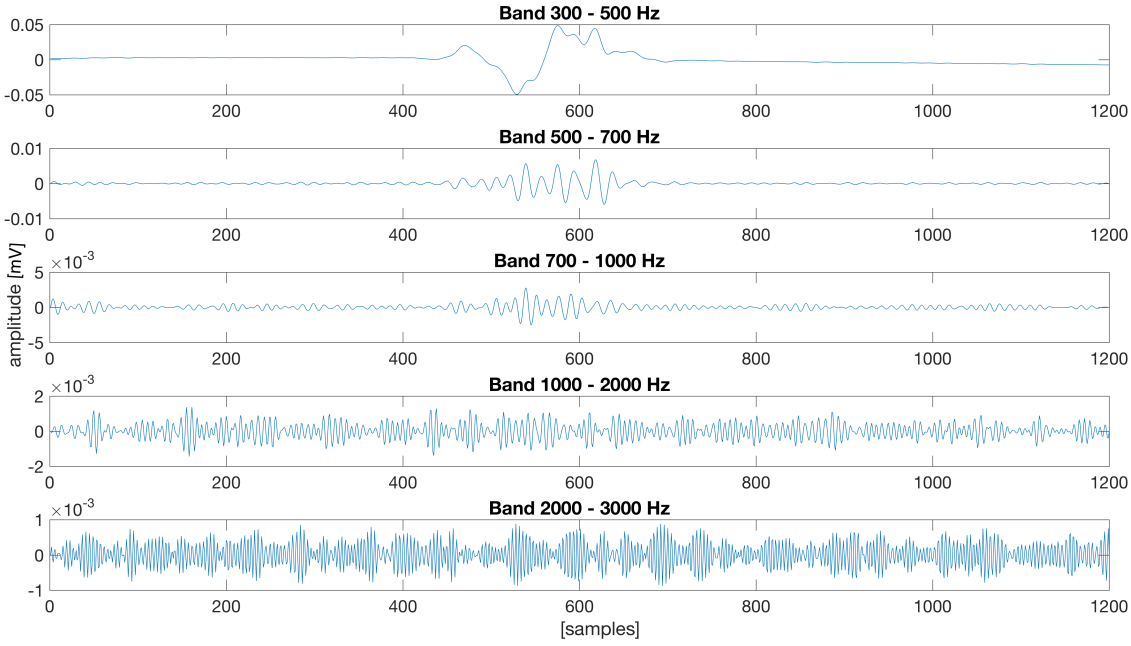

Fig. 8.13: Example of the signal decomposition.

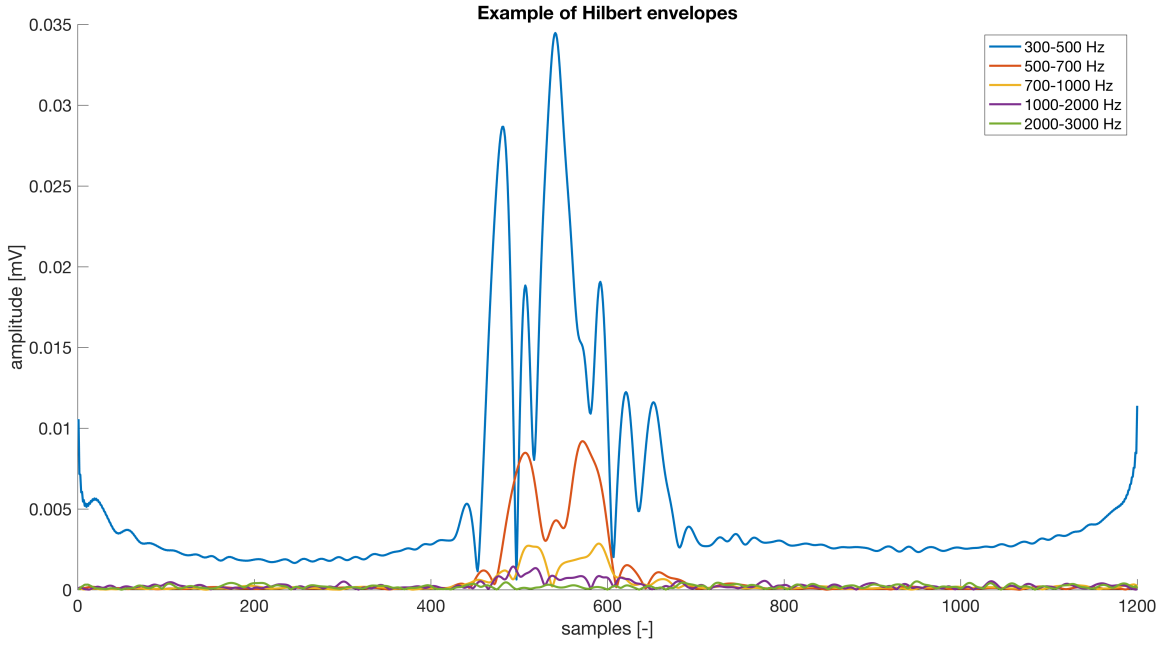

Fig. 8.14: The absolute Hilbert envelopes of 5 frequency bands example.

8.4 Detection and quantification of parameters

Quantification of the parameters, which are either the analysed parameters themselves or are the step before the computation of the actual analysed parameters, is done in the next step. In the first part there will be mentioned the maximum of the signal, the width of the envelope in respected frequency bands and RMS of the signal in significant area. In the second part we will talk about the position of the maximum of the envelope parameter.

The purpose of the function `EnvelopeDuration` is to provide exact numbers and positions of important points for every signal or envelope. What interests us the most here are the borders of the Hilbert's envelope. Those borders are used for computation of the width of the envelope as well as for limitation of the area for finding the maximum of the envelope and computing the RMS.

At the beginning, there was a manual part of the this step, where the envelope curves were examined and the aim was to find out, what is the threshold for setting up the borders of the envelope. Due to the length of the analysed signals (1200 samples, which is approximately 4 times longer then the duration of the QRS complex in rabbit heart), the value, that meets the expectations was the mean value. With this threshold, the width of the envelope was found, and area for computing RMS and finding the signal maximum was settled.

The example of settled borders and an envelope maximum can be seen at the Fig. 8.15.

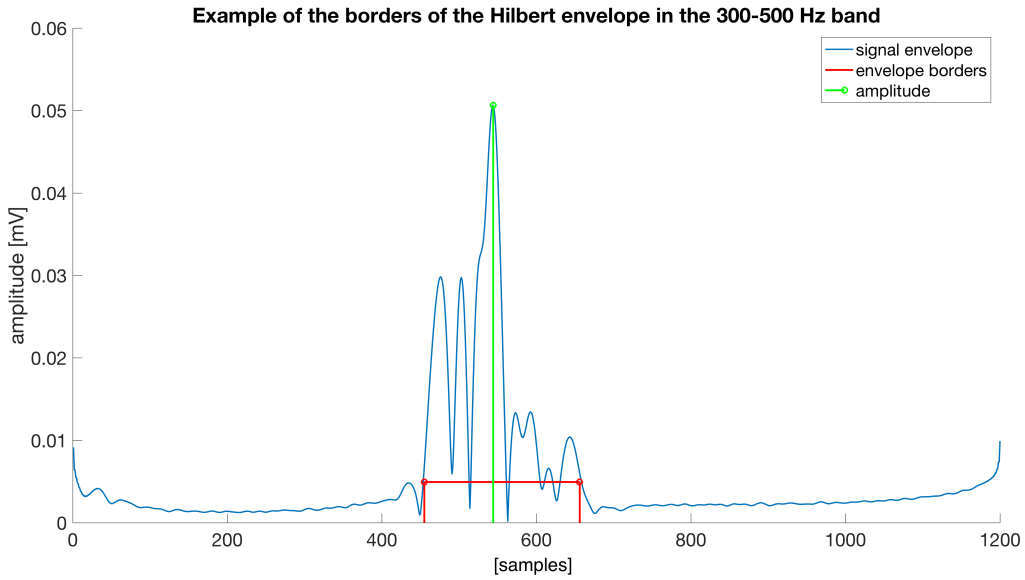

Fig. 8.15: Example of the computed envelope borders.

The parameters of signal maximum and RMS are computed in the function `amplitudeWidthRMS`. Alongside with the parameter of width of the envelope, which results are only extracted from the previous structure, the process of getting the values for these three parameters is almost identical. The equations for computing the RMS parameter was described earlier 5.1.

The most important parameter that is described in this thesis is the variability of the position of the envelope maximum with the relevance to the global position of R-wave across the analysed leads. In the study [31] is noted that the specific position of envelope's maxima in the ultra high frequency range can be addressed as a marker of ventricular dyssynchrony. Related to this, in our situation we are looking for similar connection between the position of the maximum and the propagation of AP through the ventriculus. As was mentioned, the parameter is related to the global position of R-wave. The maximum of envelope is detected and located and then computed it's relation to the position - if this result number is negative, the location of maxima is on the left side from the global position, and vice versa, when the result is a positive number, then the position lays on the right side from the global R-wave. The values of this parameter are the outcome of the script `maxPositionThroughLeads`.

The form of the structure every of the parameter values are in this phase of the analysis is the input for the statistical analysis.

8.5 Statistical evaluation

The ultimate goal of the thesis is to describe the change in HF-QRS area of ECG according to the changes in hemodynamic parameters caused by changing the inputing parameters of the perfusion system. The approach towards the statistics is based on analysing the whole set of experiments all together. Therefore, we will concentrate on the segments of the experiments, where the hemodynamic parameters are significantly changing.

8.5.1 Data distribution testing

Before the start of any statistical testing, there needs to be provided an information about the data sets' distribution. Basically, it is a test which will tell us, whether the values we are testing, in our case detected and computed parameters, are from the normal distribution. For this particular purpose there are several statistical tests, that are used for the numerical series analysis. Those are for example: one-sample Kolmogorov-Smirnov test, Anderson-Darling, Jarque-Bera test or Lilliefors test. Several of those test have been tried on the data and the outcomes of the form of boxplots, histograms and p-values have been manually reviewed. The adequate test have been the Lilliefors test and have been finally chosen for the normal distribution tests of the data.

In case the dataset is not distributed according to the Gauss curve and distribution, the data are exposed to the logarithmic transformation which can in some cases cause the distribution to become normal. If this case happens, the further analysis is done with the parametric test (as same as with the primary normal distribution) on the transformed data. If not even the transformation cause the data to gain normal distribution, the is the necessity of using non-parametric tests on original non-transformed data.

8.5.2 Significant change proving testing

With the background of the thesis the ultimate question, that is also used as the key to formulate the hypothesis for the statistical testing is - do the parameters values from the segments 'before' and 'after' the change of hemodynamic parameter come from the same distribution with the same mean value or not? The methodology of choosing the the best kind tests is very similar to the normal distribution testing and is established by it closely.

The most important information is that whether or not did data have normal distribution. If yes, original or transformed data, there is a rule of using parametric test. For this case the best choice is paired t-test. If the data are of some other

distribution, there is a need to use non-parametric test. Again, for these data is more suitable Wilcoxon test (`ranksum`).

The decision about the data testing is done automatically in the script `testovani` and all the testing is performed at the significance level of 0.05.

9 RESULTS

In this thesis is described the behaviour of the isolated rabbit heart in the perspective of mechano-electric coupling. This topic of MEC has became explored as one of the medical interests only recently. Manifestations of cardiac mechano-electric coupling are believed to play a major role in numerous clinical heart diseases. As an example can be named the lowered threshold of arrhythmia propagation that can be observed along with chamber enlargement. [32]

MEC assumes that the change of hemodynamic pressure-volumeparameters, in our case the aortic systolic pressure (ASP), aortic diastolic pressure (ADP), left ventricle end-diastolic pressure (EDP) and estimation of left ventricle flow volume (FV), will influence the heart's electrical properties.

This chapter will present the results of all the analysed data types that have been statistically tested for the evidence of significant change in ECG induced by the change of hemodynamic parameters.

9.1 Pressure and volume parameters

9.1.1 Data normality

First of all, it needs to be settled down whether or not there is a significant change in the values of pressure and volume mentioned parameters provoked by the change of two inputing parameters of preload and afterload.

In all 15 analysed experiments the sections, where do the preload and afterload change, were found. The data before the changing and after the changing have been extracted excluding the fractions of signal that stated right before or immediately after the exact position of the step to avoid the phase of stabilisation. The data were tested in 4 situations: preload increasing, preload decreasing, afterload increasing and afterload decreasing.

In the Fig. 9.1 and Fig. 9.2 can be seen the examples of distributions of aortic systolic pressure in the moment of afterload increasing and decreasing. When judging the distribution type, clearly in all presented cases the distribution is not normal. This is the fact, that appears also for the preload changing situations. From the boxplots is obvious, that the data sets suffer from numerous remote values. From histograms can be read that really, the distributions are not approaching the Gauss normal distribution. This phenomenon did not disappear even after the logaritmic transformation of the data. Therefore, the non-parametric tests have been used.

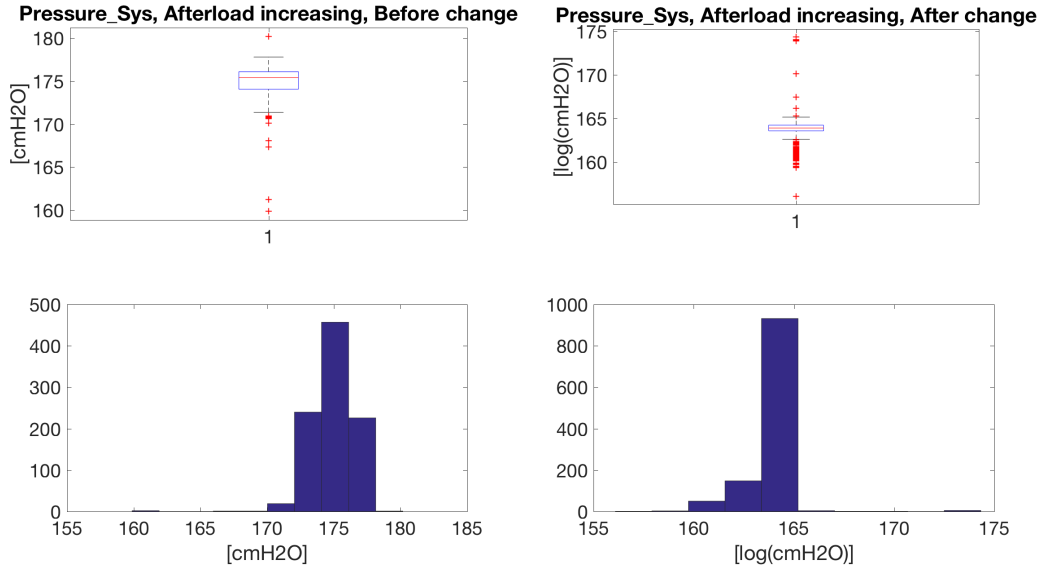

Fig. 9.1: Distribution of systolic aortic pressure in the situation of afterload increasing.

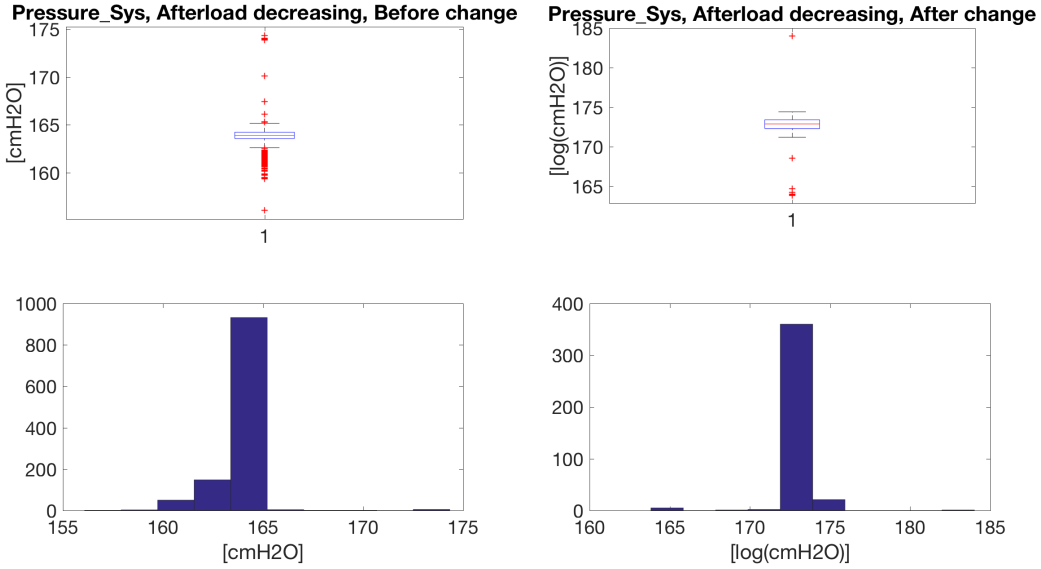

Fig. 9.2: Distribution of systolic aortic pressure in the situation of afterload increasing.

9.1.2 Parameter changing situations

Four pressure/volume parameters have been used in the thesis: aortic systolic pressure, aortic diastolic pressure, left ventricle end-diastolic pressure and estimation of left ventricle flow volume. In tables Tab. A.17, Tab. A.6, Tab. A.19 and Tab. A.20 are presented the results for lead 1 for all 4 parameters for all 4 changing situations. The rest of the results for remaining lead can be found in App. A.

All the data in tables have been tested for the zero hypothesis h0: Do the data from data groups before the parameter's change and after it come from the same distribution with the same mean value? The hypothesis has been tested at the significance level of 0.05.

For every lead and every tested situation the statistical outcome was the same - the significant difference is present in all cases. This corresponds very well with both outcomes in Fig. 9.1 and Fig. 9.2 where can be very clearly seen, mostly from the histogram, that the mean value has changed expressly. Also in presented tables most of the values are clearly different for the before/after comparison. Nevertheless, there are some cases, where the numerical outcome does not correspond with the statistical claim. E.g., in Tab. A.19 the mean values of end-diastolic pressure in afterload decreasing situation are clearly very similar to each other and even-though the statistical test says they are significantly different, from the physiological point of view, the difference of 0.3 cmH2O is not that striking. Even more questionable are the results of flow volume. The discussion whether the difference of 0.07 ml is significant or not would need to be done with specialists.

Therefore, when interpreting those statistical results, there needs to be caution and the physiological context needs to be kept in mind.

To sum it up, the heart is clearly responding to the sudden changes of preload and afterload in the pressure and volume parameters. With elevated preload, ASP is higher, which means that the heart mush have developed bigger force to eject the blood from the left ventricle to the aorta. Higher are also EDP and FV. That means, that when preload is higher, the LV does not relax as much and there is more blood in the LV. The only decreasing parameter is ADP, but on the other hand, that is lower also when preload is decreasing. For all the other mentioned parameters, the reaction to preload decreasing is exactly opposite to increasing.

When afterload is increasing, ASP, ADP and FV are all higher in their vales, the EDP is the only one with lower mean value. Thus, with increased afterload the aorta is not that relaxed, the heart needs to develop bigger force to eject blood, and there is more blood in LV. Also, with the lower EDP the LV is more relaxed. With afterload decreasing, all ASP, ADP, EDP and Fv are lower.

Tab. 9.1: The results for the change of *Pressure_Sys* according to preload and afterload, lead 1

LEAD 1	**Data before change [cmH2O]**		**Data after change [cmH2O]**	
Pressure Sys.	**Mean_Before**	**Std_Before**	**Mean_After**	**Std_After**
PreUP	161.927	8.620	164.762	7.768
PreDOWN	168.049	10.766	163.386	9.066
AfUP	165.127	7.607	183.221	10.325
AfDOWN	181.971	10.191	164.945	8.711

Tab. 9.2: The results for the change of *Pressure_Dia* according to preload and afterload, lead 1

LEAD 1	**Data before change [cmH2O]**		**Data after change [cmH2O]**	
Pressure Dia.	**Mean_Before**	**Std_Before**	**Mean_After**	**Std_After**
PreUP	86.847	5.452	84.485	5.222
PreDOWN	87.965	8.950	86.855	6.334
AfUP	84.233	5.046	100.199	11.142
AfDOWN	100.446	11.494	86.564	6.743

Tab. 9.3: The results for the change of $Pressure\_End - Dia$ according to preload and afterload, lead 1

LEAD 1	**Data before change [cmH2O]**		**Data after change [cmH2O]**	
Pressure End-Dia.	**Mean_Before**	**Std_Before**	**Mean_After**	**Std_After**
PreUP	10.496	3.288	14.062	4.074
PreDOWN	12.324	4.168	9.496	4.126
AfUP	13.399	4.077	11.585	4.095
AfDOWN	11.534	4.258	11.256	2.861

Tab. 9.4: The results for the change of $Flow\_Volume$ according to preload and afterload, lead 1

LEAD 1	**Data before change [ml]**		**Data after change [ml]**	
Flow Volume.	**Mean_Before**	**Std_Before**	**Mean_After**	**Std_After**
PreUP	0.171	0.047	0.194	0.060
PreDOWN	0.209	0.060	0.183	0.050
AfUP	0.199	0.063	0.215	0.053
AfDOWN	0.210	0.049	0.203	0.056

9.2 $HF - ECQ/HF - QRS$ parameters

With all the hemodynamic parameters reporting significant changes when the step in preload and afterload are applied, the electrical section of values is tested at all the preload/afterload changing situations. For all parameters have been computed the test of significant difference (according to their normality). At the end, there were settled the differences between the mean values and standard deviations (STDs) for every preload/afterload changing situation. The differences with STDs are, for the band 300-500 Hz, listed in tables Tab. 9.5, Tab. 9.7, Tab. 9.9 and Tab. 9.11. Their respective p-values are listed in tables Tab. 9.6, Tab. 9.8, Tab. 9.10 and Tab. 9.12.

9.2.1 Maximum of the signal

The first analysed parameter was the maximum of filtered signal. It was analysed (as same as the other parameters for above explained reasons) in 6 leads (1,2,4,6,7,8) and 3 frequency bands (300-500 Hz, 500-700 Hz, 700-1000 Hz).

According to the table with p-values (Tab. 9.6) there are cases, where the change of the preload/afterload, respectively pressure/volume, evoked the significant difference in the heart's electric response. Except for the lead 7, the rest of the leads present this kind of difference (in lead 4 it is noted, that the p-value is higher then 0.05, but with the value 0.06 it is so close to the threshold, that with the physiological context, it could be interpreted alongside with the other, significantly different leads) when preload is increasing, so when ASP, EDP and FV are increasing and ADP is decreasing. Generally, in lead 7 and lead 6 there has not been recorded any significant difference at all (with one exception in lead 6). In which direction did the change happen can be read from the table with numerical values. If the values is negative, the change of preload/ meant levelling up the parameter and vice versa„ when the difference number is positive, the change evoked lowering in the recorded parameter.

The example of the data distribution, from which have been decided the usage of parametric or non-parametric test, can be seen in Fig. 9.3.

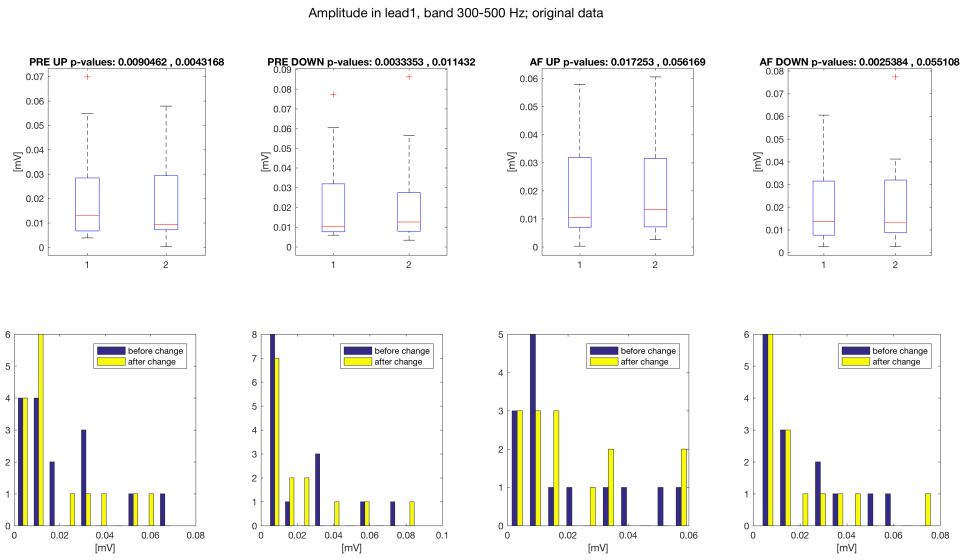

Fig. 9.3: The example of data distribution of signal maxims, band 300-500 Hz.

Tab. 9.5: Maximum of signal, band 300-500 Hz, h0: values come from the same distribution with adequate mean value

Difference [mV]	**PreUP**		**PreDOWN**		**AfUP**		**AfDOWN**	
	Mean	**Std**	**Mean**	**Std**	**Mean**	**Std**	**Mean**	**Std**
Lead 1	1.366	-0.105	-0.105	-0.002	1.527	0.262	1.442	-0.310
Lead 2	1.319	-0.117	-0.117	-0.171	1.443	0.242	1.375	-0.301
Lead 4	0.757	0.190	0.190	0.120	0.934	0.160	0.813	-0.354
Lead 6	0.473	0.060	0.060	0.002	0.739	0.410	-0.003	-0.001
Lead 7	-0.003	0.000	0.000	0.000	-0.002	0.001	-0.003	-0.001
Lead 8	-0.021	-0.001	-0.001	-0.002	-0.019	0.001	1.524	-0.097

Tab. 9.6: P-values for the maximum of signal par., band 300-500 Hz

Signal maximum band1: p-Values	**PreUP**	**PreDOWN**	**AfUP**	**AfDOWN**
Lead 1	0.0036	0.3333	0.0339	0.0247
Lead 2	0.0043	0.0699	0.0369	0.0285
Lead 4	0.0606	0.0404	0.0335	0.1016
Lead 6	0.0168	1.0000	0.3333	0.3333
Lead 7	0.3333	0.6667	0.3333	0.3333
Lead 8	0.0032	0.0153	0.0319	0.0516

9.2.2 Width of Hilbert envelope

The results interpretation for the parameter of width of Hilbert envelope is quite analogous to the maximum of the signal. Clearly, the values that do not fit in the rest of the results, are those, which are connected to the preload decreasing, so lowering all the pressure/volume parameters (ASP, ADP, EDP, FL). Also, there is surely one error in detecting the parameter itself, because for lead 2 there is a mean value 0.0707 ± 33.1633 ms, which was caused the the bad detection of the envelope border.

The most evident reactions can be observed alongside with rising preload and afterload, which in preload's case mean increased ASP, EDP and FV, decreased ADP. Similar story with afterload, rising ASP, ADP and FV, lowering EDP. During falling the preload and afterload, which have been causing lowering values in all presented pressure/volume parameters, have been significant difference noted in only 2 ou of 6 occurrences.

The example of the data distribution, from which have been decided the usage of parametric or non-parametric test, can be seen in Fig. 9.4.

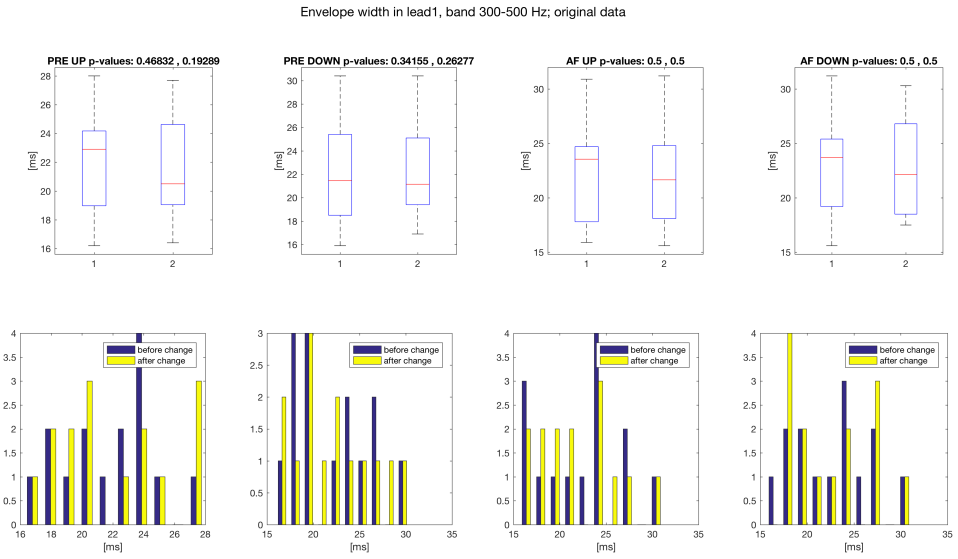

Fig. 9.4: The example of data distribution of envelope width, band 300-500 Hz.

Tab. 9.7: Hilbert envelope width, band 300-500 Hz, h0: values come from the same distribution with adequate mean value

Difference	**PreUP**		**PreDOWN**		**AfUP**		**AfDOWN**	
[sample]	**Mean**	**Std**	**Mean**	**Std**	**Mean**	**Std**	**Mean**	**Std**
Lead 1	55.0	1.414	1.414	0.707	51.0	-8.485	42.0	2.828
Lead 2	52.5	0.707	0.707	331.633	45.5	-6.364	41.5	-0.707
Lead 4	37.0	1.414	1.414	2.828	6.5	2.121	20.0	-12.728
Lead 6	78.0	11.314	11.314	0.034	86.5	6.364	81.5	-2.121
Lead 7	83.5	7.778	7.778	6.364	102.0	-2.828	92.5	-6.364
Lead 8	88.0	1.414	1.414	-9.192	75.5	-9.192	45.5	-23.335

Tab. 9.8: P-values for the width of Hilbert envelope parameter, band 300-500 Hz

Envelope width band1: p-Values	**PreUP**	**PreDOWN**	**AfUP**	**AfDOWN**
Lead 1	0.0163	0.0253	0.0218	0.3333
Lead 2	0.0037	0.3333	0.0257	0.0059
Lead 4	0.0229	0.3333	0.3333	0.3986
Lead 6	0.0117	0.3333	0.0034	0.0117
Lead 7	0.0061	0.0078	0.3333	0.3333
Lead 8	0.3333	0.0089	0.0131	0.3333

9.2.3 Root Mean Square of signal in QRS area

The RMS does not differ in its results from the previous two parameters. It also does not show any significant variation in-between the compared groups of values. As can be seen from the Tab. 9.10, the leads which have been totally resistant towards any significant difference evoked by the change of preload/afterload are lead 4 and lead 7.

In RMS, the two situation, when the system reacts more evidently, is increasing both preload and afterload, which mean with rising ASP and FV.

The example of the data distribution for RMS parameter can be seen in Fig. 9.5

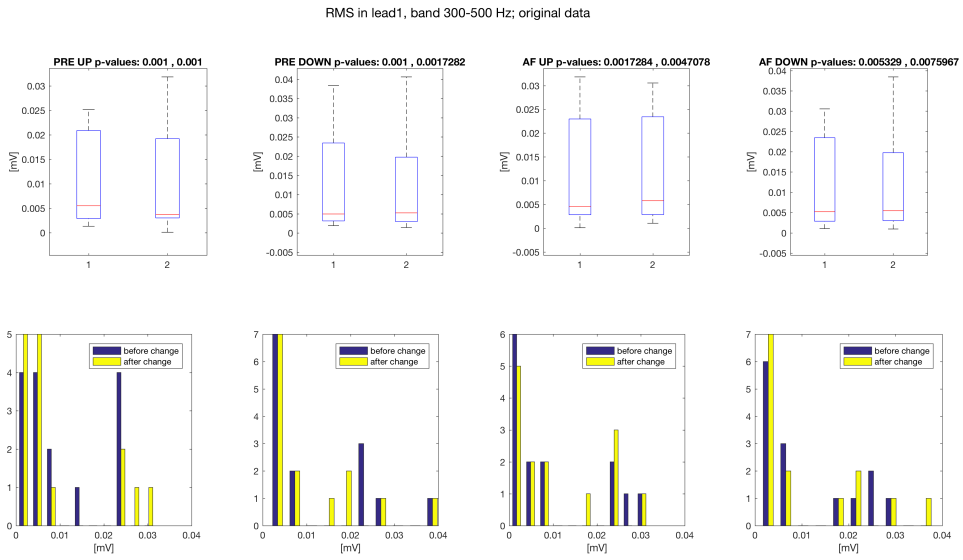

Fig. 9.5: The example of data distribution of RMS, band 300-500 Hz.

Tab. 9.9: Root mean square, band 300-500 Hz, h0: values come from the same distribution with adequate mean value

Difference [mV]	**PreUP**		**PreDOWN**		**AfUP**		**AfDOWN**	
	Mean	**Std**	**Mean**	**Std**	**Mean**	**Std**	**Mean**	**Std**
Lead 1	1.522	-0.092	-0.092	-0.005	1.555	0.185	1.496	-0.175
Lead 2	1.511	-0.090	-0.090	0.104	1.498	0.175	1.472	-0.103
Lead 4	-0.002	-0.000	-0.000	0.000	-0.001	0.000	-0.001	-0.000
Lead 6	0.500	0.048	0.048	0.000	0.778	0.414	0.954	-0.207
Lead 7	-0.001	-0.000	-0.000	0.000	-0.001	0.000	-0.001	-0.000
Lead 8	-0.010	-0.000	-0.000	-0.000	-0.008	-0.000	-0.005	-0.003

Tab. 9.10: P-values for the RMS parameter, band 300-500 Hz

RMS band1: p-Values	**PreUP**	**PreDOWN**	**AfUP**	**AfDOWN**
Lead 1	0.0021	0.0361	0.0172	0.0140
Lead 2	0.0019	0.0625	0.0167	0.0152
Lead 4	0.3333	0.3333	0.3333	0.3333
Lead 6	0.0066	1.0000	0.1394	0.0308
Lead 7	0.3333	0.6667	0.3333	0.3333
Lead 8	0.0024	0.0145	0.0380	0.1562

9.2.4 Position of envelope maximum in relation with global R-wave position

The propagation of the action potential can be observed throughout the separate leads. When the healthy heart is observed, the position of the maximum of envelope is stable within the lead and the successive order of the leads. The change in the pattern as a result of the change of input parameters is an evidence of the heart's reaction. If there is an evident prolongation or shortening in propagation between leads in the following experiment phases, by addressing the specific leads it can be found which part of heart was influenced.

In the Fig. 9.6, Fig. 9.7 and Fig. 9.8 are presented an examples of different positions of maxims in 6 different leads within one experimental phase in three frequency bands. As can be seen, the sequence of leads in that exact moment from left to right is: $8 \rightarrow 1 \rightarrow 2 \rightarrow 4 \rightarrow 7 \rightarrow 6$ and obviously, this order keeps up in the three frequency bands.

From Tab. 9.12 is evident, that the change of input parameter do have a different effect on different parts of the heart. In leads 1 and 2, it is clear, that the position of the envelope maximum is stable and does not change with the different pressure or volume conditions. From lead 4, the change of parameter has greater effect on the maximum position. How the position and in which direction around the global R-wave is moving can be seen in the Tab. 9.11.

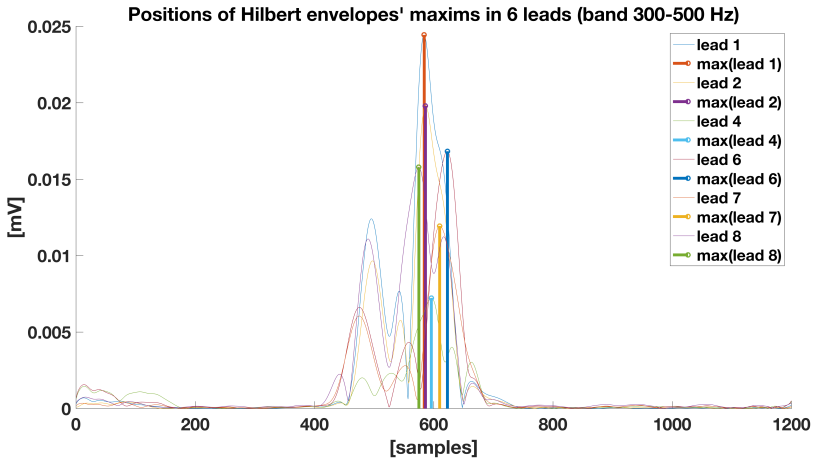

Fig. 9.6: The positions of Hilbert envelopes' maxims in one section if experiment in all analysed leads.

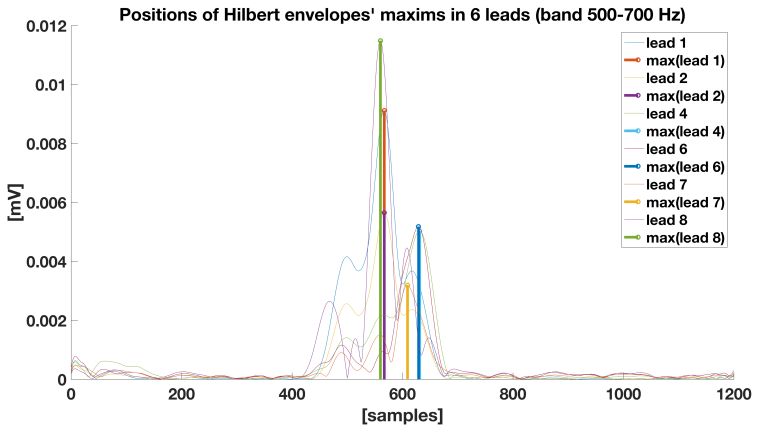

Fig. 9.7: The positions of Hilbert envelopes' maxims in one section if experiment in all analysed leads.

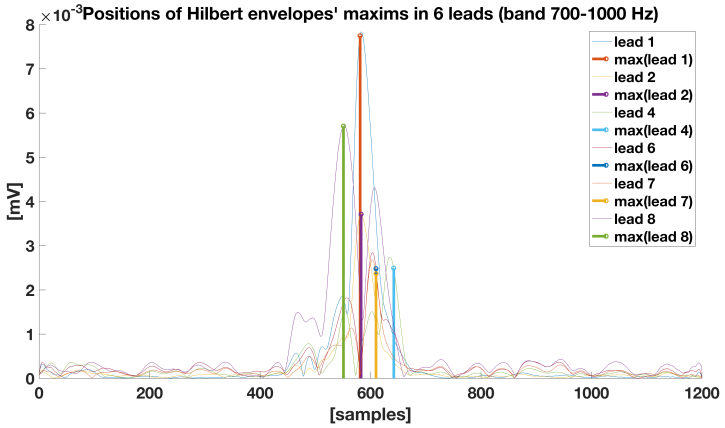

Fig. 9.8: The positions of Hilbert envelopes' maxims in one section if experiment in all analysed leads.

In the tables bellow (Tab. 9.11 and Tab. 9.12) are listed the result for the question: did the position on the envelope's maximum move in respected leads, when the input parameters have changed? Yes, it mostly did.

Tab. 9.11: Envelope maximum position, band 300-500 Hz, h0: values come from the same distribution with adequate mean value

Difference	**PreUP**		**PreDOWN**		**AfUP**		**AfDOWN**	
[sample]	**Mean**	**Std**	**Mean**	**Std**	**Mean**	**Std**	**Mean**	**Std**
Lead 1	-13.5	7.071	7.071	-1.414	-93.5	104.652	-92.5	102.530
Lead 2	-12.5	5.657	5.657	313.955	-94.0	103.238	-93.5	99.702
Lead 4	-27.0	62.225	62.225	1.414	-66.0	5.657	-70.0	4.243
Lead 6	32.5	3.536	3.536	-1.414	-1.368	-0.026	-5.0	-52.326
Lead 7	26.5	2.121	2.121	-0.707	31.0	-1.414	26.5	0.707
Lead 8	7.0	0.000	0.000	-2.121	-0.099	0.100	-2.0	2.828

Tab. 9.12: P-values for the position of the envelope maximum, band 300-500 Hz

Maximum position band1: p-Values	**PreUP**	**PreDOWN**	**AfUP**	**AfDOWN**
Lead 1	0.2161	0.0700	0.3333	0.3507
Lead 2	0.1699	0.3333	0.3333	0.3394
Lead 4	1.0000	0.0006	0.0091	0.0035
Lead 6	0.0123	0.0028	0.3333	1.0000
Lead 7	0.0156	0.0035	0.0026	0.0046
Lead 8	0.1318	0.0434	0.5043	1.0000

10 DISCUSSION

The design of the analysis was created according to available literature and individual experiences. However, there are facts that need to be considered when construing the outcomes.

First of all, this analysis stand by the results on its own without other studies to lean on. There are no officially published reference studies which would describe the high-frequency analysis of ECG data from isolated rabbit heart. Some steps of the analysis have used manual subjective approach and therefore, in case of similar analysis, the research for potential updated information in the expert circles is recommended.

Second important fact to keep in mind is, that the study applies the global point of view on the data. The clustering process included sorting data according to its resemblance and morphological closeness, which required choosing data from the experimental phases in a way to avoid big differences between individual beats. Because of that, neither beats from the beginning or the end of the separated experimental phase have been included into created clusters. On the other hand, exactly those beats immediately following the sudden step could describe the process of heart's electrical adaptation most precisely. Therefore, local approach towards considered data, which might be hiding some interesting facts about isolated rabbit heart's MEC, is meant to be a genuine idea for further analysis as a sequel to this master's thesis.

And finally, in the author's eyes the most important not to forget about information, is the physiological conditions and interpretation, what the gained values actually mean in the terms of hemodynamic parameters. As was mentioned earlier, there is a possibility of statistical test results in saying that, yes, in this situation the p-value is smaller then 0.05 and the significant difference is present. However, if we actually look at the particular parameters values, we can find out, that even-though the test says so, the actual state of system is not so different.

On a few previous pages have been presented the results of the high-frequency analysis. When the results covering the pressure/volume reactions on the sudden changes according to the input parameters, preload and afterload, are summarised, it has to be stated, that from the statistical point of view in the band 300-500 Hz, where the majority of information is present, did appear significant difference between the data before the change and after it in all cases. When considering the outcomes of electrical parameters analysis, the significant difference does not appear in all the cases, but in the reasonably high amount of them. The exception are present in all the parameters' data, but all together, the reaction happened in more cases then not.

One of the reasons, why there are no significantly shown changes in some cases, might be the number of beats entering the averaging process. Even-though the criterion for resemblance between two supposedly same beats is high, the fixed established number of beats included in one morphological group could result in even higher precision with cross-correlation. It suits to add here, that the difference between the sizes of individual morphological clusters representing experimental phases differs between experiments with big variance (mostly due to used protocol).

To apply all mentioned possible lacks in this study, the analysis would need to be performed mostly manually with high emphasis on location precision. On the other hand, the results of this way performed analysis would have been great reference results for any subsequent analysis.

11 CONCLUSION

Master's thesis, which you have just read, deals with the problematics of HF-ECG and HF-QRS analysis in the isolated rabbit heart. During devising the thesis, the not automatic programme has for the analysis has been developed in the programming environment of MATLAB (ver. 2016a, macOS Sierra 10.12.4). All the code is a part of included DVD, table of content in App.C.

The thesis itself consists of two main parts. The first one, literature review, covers the topic from the theoretic point of view. The formation of ECG, as in action potential, genesis of the ECG and recording ECG are explained. The chapter about mechano-electric coupling supplies the information about how the electric mechanism of heart reacts to the mechanical initiative. As one of the main instruments for realization the thesis the signal averaging was chosen, the chapter with this name consists of information about basics and methods of the process. At the end, the properties, system requirements and analysis methods for HF-QRS and HF-ECG are described.

The second big part of the thesis is the practical application. The aim of the study was to prepare the data and design and perform the analysis for the provided signals. Firstly, the experimental data are introduced - how they were acquired, what system has been used for measuring, description of the experimental protocols and which signals are included in every data set are all included in the Experimental data chapter. The thesis initiated with the ambition to analyse all the parameters in 5 different frequency bands (Tab. 8.1). However, the signal decomposition outcomes showed, that the last two bands do not, at the moment, provide any additional interesting information, are consist mostly of noise and were excluded from the analysis. Therefore, the rest of the analysis was performed on 3 frequency bands: 300-500 Hz, 500-700 Hz, 700-1000 Hz. The reason, why there have not been computed the variant of analysis with different frequency bands is mostly from time reasons. The presented bands have served well in this case and therefore, the results are interpreted according to them. Nevertheless, the idea of finding the best frequency band suitable for HF-ECG analysis in isolated rabbit heart could be a very interesting topic for following work.

With frequency bands stated, the thesis continues in description of the used methods. The biggest part of the preprocessing step and data preparation were clustering and signal averaging. Clustering sorted the data according to the experimental phase (manual) and according to the morphological outline of the complex (automatic). The purpose of the step was to create the groups of signal extractions, which are very similar (crosscorrelation coefficient higher then 0.985) and therefore they represent the stable phase of the signal. Every one of those groups were then

averaged with the target to gain signal-to-noise ratio (SNR). The product of averaging process are experiments which individual phases are described each by averaged beat in leads 1, 2, 4, 6, 7 and 8, the indexes of the beats within the experimental phase, that have been included in the morphological group, and the signal parts themselves.

The averaged beats then enter the signal decomposition step where they have been filtered with listed filters. After, the chosen parameters can be detected and quantified. Data, that have been used, are the sets of pressure (ASP, ADP, EDP) and volume (FV) signals, and 6 channels of ECG. On pressure/volume data have been analysed the aortic systolic pressure, aortic diastolic pressure, end diastolic pressure and estimation of flow volume, all in the relation with the left ventricle. In the ECG data, filtered signal maximum, Hilbert envelope width, RMS of filtered signal in QRS area and position of Hilbert envelope maximum have been analysed.

All the programs that have been used for the analysis are enclosed with this thesis and the list of enclosed files can be found in App.AppC. To go through the whole analysis process it is recommended to follow steps in the script `DP_WHOLE_PROGRAM.m`. The automatic detection and estimation of analysed parameters is realised in scripts: `DP_amplitudeWidthRMS.m`, `DP_maxPositionThroughLeads.m` and `DP_PressVol_sort.m`.

All in all, it can be stated, that the reactions of the system on step changes in input parameters from the MEC point of view are definitely present in the signals. Increasing preload results in left ventricle's need to provide bigger force to eject the blood into the aorta, it does not relax as much and the volume of blood in LV is higher. On the other hand, when preload is lowered, all the pressure and volume parameters are smaller. That applies also for the lowering of afterload, though, when afterload is rising, the LV reacts with lower EDP and higher ASP, ADP and FV. Also, for the HF-QRS and HF-ECG parameters the reactions are present. Mostly, the electrical actions of the heart react to the elevation of systolic pressure and the volume of blood in left ventricle.

As much as the thesis has been constructed with the best intentions and clear goal, there are several facts, which, when applied, could improve the methodology. One possible uplift would be to perform the analysis with the focus on local changes more than global ones. In this thesis, the parts of the signals surrounding the exact spot os the step change have been excluded. Therefore, analysis with the focus on those excluded parts could be interesting. The precise number of beats included in one morphological group could also be an improvement in the morphological precision. The last but not the least important fact to mention is, that the thesis itself is self-prooving in the concept of comparing results with previously held studies.

BIBLIOGRAPHY

[1] DESPOPOULOS, Agamemnon and Stefan SILBERNAGL. Color atlas of physiology. 5th ed. Stuttgart: Thieme, 2000. ISBN 15-889-0061-4.

[2] MALMIVUO, Jaakko. and Robert. PLONSEY. 1995. Bioelectromagnetism: principles and applications of bioelectric and biomagnetic fields. New York: Oxford University Press. ISBN 01-950-5823-2.

[3] MADIAS, John E. 2013. A Proposal for a 9-Lead Electrocardiogram Recorded via the Wilson's Central Terminal. Annals of Noninvasive Electrocardiology. 18(2), 103-106. ISSN 1082720x. Dostupné také z: http://doi.wiley.com/10.1111/anec.12040

[4] DUPRE, Anthony, Sarah VINCENT and Paul A. IAIZZO. 2005. Basic ECG Theory, Recordings, and Interpretation. Handbook of Cardiac Anatomy, Physiology, and Devices. Totowa, NJ: Humana Press, , 191. DOI: 10.1007/978159259835915. ISBN 9781588294432.

[5] SÖRNMO, Leif and Pablo LAGUNA. c2005. Bioelectrical signal processing in cardiac and neurological applications. Burlington: Elsevier Academic Press. ISBN $978-0-12-437552-9$.

[6] PFEIFFER, Emily R., Jared R. TANGNEY, Jeffrey H. OMENS a Andrew D. MCCULLOCH, 2014. Biomechanics of Cardiac Electromechanical Coupling and Mechanoelectric Feedback. Journal of Biomechanical Engineering. (136). DOI: 10.1115/1.4026221. ISBN 10.1115/1.4026221.

[7] QUINN, T. Alexander, 2015. Cardiac mechano-electric coupling: a role in regulating normal function of the heart? Cardiovascular Research. (108), 1-3. DOI: $10.1093/cvr/cvv203$. ISBN $10.1093/cvr/cvv203$.

[8] PETTERSSON, Jonas D., Elena D. CARRO, Lars D. EDENBRANDT, et al. Spatial, individual, and temporal variation of the high-frequency QRS amplitudes in the 12 standard electrocardiographic leads. DOI: $10.1067/mhj.2000.101782$. ISBN $10.1067/mhj.2000.101782$.

[9] GOMES, J. Anthony. c1993. The signal averaged ECG: a historical perspective. Signal averaged electrocardiography: concepts, methods, and applications. Boston: Kluwer Academic Publishers. ISBN 0792323904.

[10] BERBARI, Edward J. a Paul LANDER. 1993. The methods of recording and analysis of the signal averaged ECG. , pp 49-68. DOI: $10.1007/978-94-011-0894-2_4$. ISBN $10.1007/978-94-011-0894-2_4$.

[11] GOMES, J. Anthony. The vector magnitude, time domain analysis and standards for late potentials. DOI: 10.1007/978 − 94 − 011 − 0894 − 2_5. ISBN 10.1007/978 − 94 − 011 − 0894 − 2_5.

[12] SIMSON, M. B. 1981. Use of signals in the terminal QRS complex to identify patients with ventricular tachycardia after myocardial infarction. Circulation. 64(2), pp 235-242. DOI: 10.1161/01.CIR.64.2.235. ISBN 10.1161/01.CIR.64.2.235.

[13] MACHAC, Josef a J. Anthony GOMES. 1993. Frequency domain analysis. , pp. 81-123. DOI: 10.1007/978 − 94 − 011 − 0894 − 2_6. ISBN 10.1007/978 − 94 − 011 − 0894 − 2_6.

[14] TRÄGARDH, Elin and Todd T. SCHLEGEL. 2007. High-frequency QRS electrocardiogram. Clin Physiol Funct Imaging. 27, pp 197-204. DOI: 10.1111/j.1475 − 097X.2007.00738.x. ISBN 10.1111/j.1475 − 097X.2007.00738.x.

[15] MERX, Marc W., Jürgen SCHRADER, Adam SZELĄG a Richard SCHULZ. 2005. The Working Heart. Practical Methods in Cardiovascular Research. , pp 173-189. DOI: 10.1007/3−540−26574−$0_1$0. ISBN 10.1007/3−540−26574−$0_1$0.

[16] VINCENT, Jean-Louis, 2008. Understanding cardiac output. Critical care [online]. 12(4)(174) [cit. 2017-05-17]. DOI: 10.1186/cc6975. ISBN 10.1186/cc6975.

[17] HOLZHEIMER, René G. a John A. MANNICK, 2001. Surgical Treatment: Evidence-based and Problem-oriented. 1. Munich: Zuckschwerdt. ISBN 9783886037148.

[18] GOLDBERGER, A. L., V. BHARGAVA, V. FROELICHER a J. COVELL. 1981. Effect of myocardial infarction on high-frequency QRS potentials. Circulation. 64(1), pp 34-42. DOI: 10.1161/01.CIR.64.1.34. ISBN 10.1161/01.CIR.64.1.34.

[19] BREITHARDT, Günter, Michael E. CAIN, Nabil EL-SHERIF, Nancy C. FLOWERS, Vinzenz HOMBACH, Michiel JANSE, Michael B. SIMSON a Gerhard STEINBECK. 1991. Standards for analysis of ventricular late potentials using high-resolution or signal-averaged electrocardiography: A statement by a task force committee of the European Society of Cardiology, the American Heart Association, and the American College of Cardiology. Circulation. 83(4), pp 1481-1488. DOI: 10.1016/0735 − 1097(91)90822 − Q. ISBN 10.1016/0735 − 1097(91)90822 − Q.

[20] HEJČ, Jakub., RONZHINA, M., JANOUŠEK, O., OLEJNÍČKOVÁ, V., NOVÁKOVÁ, M., KOLÁŘOVÁ, J., STRAČINA, T. The Response of Ventricular Repolarization Parameters to Preload Changes in the Isolated Working Heart. In Computing in Cardiology 2016. Computers in Cardiology. 43. Vancouver, Canada: Computing in Cardiology 2016, 2016. s. 1-4. ISBN: $978-1-5090-0684-7$. ISSN: $0276-6574$

[21] HEJČ, Jakub, RONZHINA, M., JANOUŠEK, O., OLEJNÍČKOVÁ, V., NOVÁKOVÁ, M., KOLÁŘOVÁ, J. The Effect of Heart Orientation on High Frequency QRS Components in Multiple Bandwidths. In Computing in Cardiology 2015. 42. Nice, France: Computing in Cardiology 2015, 2015. s. 1121-1124. ISBN: $978-1-4799-4347-0$.

[22] RONZHINA, Marina, JANOUŠEK, O., SCHEER, P., NOVÁKOVÁ, M., PROVAZNÍK, I., and KOLÁŘOVÁ, J.,. Determination of the Frequency Bands for Heart Rate Variability: Studies on the Intact and Isolated Rabbit Hearts. Computing in Cardiology, Belfast, UK: IEEE, 2010, roč. 37, č. 1, s. 927-930. ISSN $0276-6574$.

[23] RONZHINA, Marina, POTOČŇÁK, T., JANOUŠEK, O., KOLÁŘOVÁ, J., NOVÁKOVÁ, M. and PROVAZNÍK, I.. Spectral and Higher-Order Statistical Analysis of the ECG: Application to the Study of Ischemia in Rabbit Isolated Hearts. In Alan Murray. Computing in Cardiology. Krakow: Computing in Cardiology, 2012. s. 645-648, 4 s. ISBN $978-1-4673-2074-0$.

[24] JANOUŠEK, Oto, Marina RONZHINA, Peter SCHEER, Marie NOVÁKOVÁ, Ivo PROVAZNÍK a Jana KOLÁŘOVÁ. HRV in Isolated Rabbit Hearts and in vivo Rabbit Hearts. Computing in Cardiology, Belfast, UK: IEEE, 2010, roč. 37, č. 1, s. 923-926. ISSN $0276-6574$.

[25] CHEN, J., R. MANDAPATI, O. BERENFELD, A. C. SKANES a J. JALIFE. 2000. High-Frequency Periodic Sources Underlie Ventricular Fibrillation in the Isolated Rabbit Heart. Circulation research. 86(1), pp 86-93. DOI: $10.1161/01.RES.86.1.86$. ISBN $10.1161/01.RES.86.1.86$.

[26] LOLOV, V. R. and R. V. LOLOV. 1985. Spectral analysis of the normal electrocardiogram of rabbits. Basic Research in Cardiology. 80(4), pp 353–356. DOI: $10.1007/BF01908178$. ISBN $10.1007/BF01908178$.

[27] KOUR, J., AHMED J. A., and O. AARIF. 2013. Impact of Heat Stress on Electrocardiographic Changes in New Zealand White Rabbits. Journal of Stress Physiology & Biochemistry. 9(2), pp. 242-252.

[28] HEJČ, Jakub, Martin VÍTEK, Marina RONZHINA, Marie NOVÁKOVÁ a Jana KOLÁŘOVÁ. 2015. A Wavelet-Based ECG Delineation Method: Adaptation to an Experimental Electrograms with Manifested Global Ischemia. Cardiovascular Engineering and Technology. 6(3), pp 364–375. DOI: $10.1007/s13239-015-0224-z$. ISBN $10.1007/s13239-015-0224-z$.

[29] PLESINGER, Filip, Juraj JURCO, Josef HALAMEK, Pavel LEINVEBER, T. REICHLOVA a Pavel JURAK. Multichannel QRS Morphology Clustering - Data Preprocessing for Ultra-High-Frequency ECG Analysis. DOI: 10.5220/0005604200110019. ISBN 10.5220/0005604200110019.

[30] QUINN, T. Alexander a Peter KOHL. 2016. Rabbit models of cardiac mechano-electric and mechano-mechanical coupling. Progress in Biophysics and Molecular Biology. 121(2), pp 110-122. DOI: $10.1016/j.pbiomolbio.2016.05.003$. ISBN $10.1016/j.pbiomolbio.2016.05.003$.

[31] JURAK, Pavel, Josef HALAMEK, Filip PLESINGER, Tereza REICHLOVA, Jolana LIPOLDOVA, Miroslav NOVAK, Katerina JURAKOVA a Pavel LEINVEBER, 2015. An additional marker of ventricular dyssynchrony. In: Computing in Cardiology 2015. Nice, France: IEEE. DOI: $10.1109/CIC.2015.7408590$. ISBN $978-1-5090-0684-7$. ISSN $2325-887X$.

[32] KOHL, Peter, Frederick SACHS a Michael R. FRANZ, 2011. Cardiac Mechano-Electric Coupling and Arrhythmias. 2. New York, United States: Oxford University Press. ISBN $978-0-19-957016-4$.

LIST OF SYMBOLS, PHYSICAL CONSTANTS AND ABBREVIATIONS

ECG electrocardiogram

HF high frequency

SAN sino-atrial node

AVN atrio-ventricular node

AP action potential

EA electrical activation

RMS root mean square

ASP aortic systolic pressure

ADP aortic diastolic pressure

EDP end-diastolic pressure

FV flow volume

QRS QRS complex

LV left ventricle

LA left atrium

FIR filter with finite impulse response

IIR filter with infinite impulse response

LIST OF APPENDICES

A RESULTS FOR PRESSURE/VOLUME STATISTICS

Tab. A.1: The results for the change of *Pressure_Sys* according to preload and afterload, lead 2

LEAD 2	**Data before change [cmH2O]**		**Data after change [cmH2O]**	
Pressure Sys.	**Mean_Before**	**Std_Before**	**Mean_After**	**Std_After**
PreUP	161.945	8.606	164.846	7.712
PreDOWN	168.080	10.737	163.398	9.060
AfUP	165.205	7.546	183.125	10.421
AfDOWN	181.990	10.169	164.972	8.689

Tab. A.2: The results for the change of *Pressure_Dia* according to preload and afterload, lead 2

LEAD 2	**Data before change [cmH2O]**		**Data after change [cmH2O]**	
Pressure Dia.	**Mean_Before**	**Std_Before**	**Mean_After**	**Std_After**
PreUP	86.841	5.448	84.443	5.203
PreDOWN	87.941	8.943	86.850	6.328
AfUP	84.195	5.024	100.091	11.277
AfDOWN	100.481	11.458	86.540	6.727

Tab. A.3: The results for the change of $Pressure\_End - Dia$ according to preload and afterload, lead 2

LEAD 2	**Data before change [cmH2O]**		**Data after change [cmH2O]**	
Pressure End-Dia.	**Mean_Before**	**Std_Before**	**Mean_After**	**Std_After**
PreUP	10.498	3.289	14.080	4.074
PreDOWN	12.325	4.167	9.493	4.125
AfUP	13.414	4.078	11.616	4.149
AfDOWN	11.519	4.246	11.26	2.862

Tab. A.4: The results for the change of $Flow\_Volume$ according to preload and afterload, lead 2

LEAD 2	**Data before change [ml]**		**Data after change [ml]**	
Flow Volume.	**Mean_Before**	**Std_Before**	**Mean_After**	**Std_After**
PreUP	0.171	0.047	0.194	0.060
PreDOWN	0.210	0.060	0.183	0.050
AfUP	0.199	0.063	0.215	0.053
AfDOWN	0.211	0.049	0.203	0.056

Tab. A.5: The results for the change of $Pressure\_Sys$ according to preload and afterload, lead 4

LEAD 4	**Data before change [cmH2O]**		**Data after change [cmH2O]**	
Pressure Sys.	**Mean_Before**	**Std_Before**	**Mean_After**	**Std_After**
PreUP	161.935	8.627	164.807	7.765
PreDOWN	168.028	10.758	163.384	9.065
AfUP	165.180	7.592	183.094	10.294
AfDOWN	182.059	10.032	164.953	8.727

Tab. A.6: The results for the change of $Pressure\_Dia$ according to preload and afterload, lead 4

LEAD 4	**Data before change [cmH2O]**		**Data after change [cmH2O]**	
Pressure Dia.	**Mean_Before**	**Std_Before**	**Mean_After**	**Std_After**
PreUP	86.843	5.451	84.461	5.223
PreDOWN	87.929	8.936	86.849	6.331
AfUP	84.202	5.041	100.198	11.189
AfDOWN	100.651	11.228	86.566	6.766

Tab. A.7: The results for the change of $Pressure\_End - Dia$ according to preload and afterload, lead 4

LEAD 4	**Data before change [cmH2O]**		**Data after change [cmH2O]**	
Pressure End-Dia.	**Mean_Before**	**Std_Before**	**Mean_After**	**Std_After**
PreUP	10.498	3.292	14.082	4.073
PreDOWN	12.339	4.165	9.501	4.118
AfUP	13.409	4.082	11.625	4.089
AfDOWN	11.481	4.144	11.267	2.861

Tab. A.8: The results for the change of $Flow\_Volume$ according to preload and afterload, lead 4

LEAD 4	**Data before change [ml]**		**Data after change [ml]**	
Flow Volume.	**Mean_Before**	**Std_Before**	**Mean_After**	**Std_After**
PreUP	0.171	0.047	0.194	0.060
PreDOWN	0.210	0.060	0.183	0.050
AfUP	0.200	0.062	0.215	0.053
AfDOWN	0.212	0.048	0.203	0.056

Tab. A.9: The results for the change of $Pressure\_Sys$ according to preload and afterload, lead 6

LEAD 6	**Data before change [cmH2O]**		**Data after change [cmH2O]**	
Pressure Sys.	**Mean_Before**	**Std_Before**	**Mean_After**	**Std_After**
PreUP	161.924	8.619	164.759	7.769
PreDOWN	168.024	10.745	163.393	9.056
AfUP	165.130	7.600	183.200	10.304
AfDOWN	182.185	10.055	164.954	8.715

Tab. A.10: The results for the change of $Pressure\_Dia$ according to preload and afterload, lead 6

LEAD 6	**Data before change [cmH2O]**		**Data after change [cmH2O]**	
Pressure Dia.	**Mean_Before**	**Std_Before**	**Mean_After**	**Std_After**
PreUP	86.841	5.448	84.443	5.203
PreDOWN	87.941	8.943	86.850	6.328
AfUP	84.195	5.024	100.091	11.277
AfDOWN	100.481	11.458	86.540	6.727

Tab. A.11: The results for the change of $Pressure\_End-Dia$ according to preload and afterload, lead 6

LEAD 6	**Data before change [cmH2O]**		**Data after change [cmH2O]**	
Pressure End-Dia.	**Mean_Before**	**Std_Before**	**Mean_After**	**Std_After**
PreUP	86.852	5.449	84.491	5.220
PreDOWN	87.949	8.928	86.849	6.325
AfUP	84.233	5.040	100.222	11.131
AfDOWN	100.672	11.164	86.572	6.756

Tab. A.12: The results for the change of *Flow_Volume* according to preload and afterload, lead 6

LEAD 6	**Data before change [ml]**		**Data after change [ml]**	
Flow Volume.	**Mean_Before**	**Std_Before**	**Mean_After**	**Std_After**
PreUP	0.171	0.047	0.194	0.060
PreDOWN	0.210	0.060	0.183	0.050
AfUP	0.199	0.063	0.215	0.053
AfDOWN	0.212	0.048	0.203	0.056

Tab. A.13: The results for the change of *Pressure_Sys* according to preload and afterload, lead 7

LEAD 7	**Data before change [cmH2O]**		**Data after change [cmH2O]**	
Pressure Sys.	**Mean_Before**	**Std_Before**	**Mean_After**	**Std_After**
PreUP	161.924	8.620	164.753	7.770
PreDOWN	168.029	10.755	163.386	9.060
AfUP	165.124	7.599	183.227	10.310
AfDOWN	182.214	10.065	164.955	8.715

Tab. A.14: The results for the change of *Pressure_Dia* according to preload and afterload, lead 7

LEAD 7	**Data before change [cmH2O]**		**Data after change [cmH2O]**	
Pressure Dia.	**Mean_Before**	**Std_Before**	**Mean_After**	**Std_After**
PreUP	86.851	5.451	84.494	5.222
PreDOWN	87.963	8.934	86.855	6.328
AfUP	84.236	5.041	100.225	11.123
AfDOWN	100.673	11.156	86.572	6.756

Tab. A.15: The results for the change of $Pressure\_End-Dia$ according to preload and afterload, lead 7

LEAD 7	**Data before change [cmH2O]**		**Data after change [cmH2O]**	
Pressure End-Dia.	**Mean_Before**	**Std_Before**	**Mean_After**	**Std_After**
PreUP	10.496	3.289	14.053	4.074
PreDOWN	12.309	4.159	9.482	4.119
AfUP	13.387	4.079	11.571	4.085
AfDOWN	11.428	4.136	11.255	2.860

Tab. A.16: The results for the change of *Flow_Volume* according to preload and afterload, lead 7

LEAD 7	**Data before change [ml]**		**Data after change [ml]**	
Flow Volume.	**Mean_Before**	**Std_Before**	**Mean_After**	**Std_After**
PreUP	0.171	0.047	0.194	0.060
PreDOWN	0.210	0.060	0.183	0.050
AfUP	0.199	0.063	0.215	0.053
AfDOWN	0.213	0.048	0.203	0.056

Tab. A.17: The results for the change of *Pressure_Sys* according to preload and afterload, lead 8

LEAD 8	**Data before change [cmH2O]**		**Data after change [cmH2O]**	
Pressure Sys.	**Mean_Before**	**Std_Before**	**Mean_After**	**Std_After**
PreUP	161.925	8.615	164.761	7.769
PreDOWN	168.029	10.744	163.393	9.057
AfUP	165.130	7.601	183.082	10.391
AfDOWN	182.216	10.066	164.888	8.709

Tab. A.18: The results for the change of *Pressure_Dia* according to preload and afterload, lead 8

LEAD 8	**Data before change [cmH2O]**		**Data after change [cmH2O]**	
Pressure Dia.	**Mean_Before**	**Std_Before**	**Mean_After**	**Std_After**
PreUP	86.850	5.449	84.49	5.220
PreDOWN	87.948	8.930	86.849	6.327
AfUP	84.234	5.041	100.150	11.259
AfDOWN	100.666	11.157	86.463	6.568

Tab. A.19: The results for the change of $Pressure\_End-Dia$ according to preload and afterload, lead 8

LEAD 8	**Data before change [cmH2O]**		**Data after change [cmH2O]**	
Pressure End-Dia.	**Mean_Before**	**Std_Before**	**Mean_After**	**Std_After**
PreUP	10.496	3.290	14.057	4.072
PreDOWN	12.319	4.160	9.490	4.123
AfUP	13.391	4.077	11.599	4.139
AfDOWN	11.433	4.138	11.269	2.866

Tab. A.20: The results for the change of $Flow\_Volume$ according to preload and afterload, lead 8

LEAD 8	**Data before change [ml]**		**Data after change [ml]**	
Flow Volume.	**Mean_Before**	**Std_Before**	**Mean_After**	**Std_After**
PreUP	0.171	0.047	0.194	0.060
PreDOWN	0.210	0.060	0.183	0.050
AfUP	0.199	0.063	0.214	0.053
AfDOWN	0.212	0.048	0.202	0.056

B RESULTS FOR ELECTRICAL PARAMETERS STATISTICS

Tab. B.1: Maximum of signal, band 500-700 Hz, h0: values come from the same distribution with adequate mean value

Difference [mV]	PreUP		PreDOWN		AfUP		AfDOWN	
	Mean	Std	Mean	Std	Mean	Std	Mean	Std
Lead 1	-0.004	-0.001	-0.001	-0.001	-0.006	-0.001	-0.003	-0.002
Lead 2	1.585	-0.018	-0.018	0.001	-0.003	-0.001	-0.002	-0.001
Lead 4	-0.001	-0.000	-0.000	0.299	1.196	0.373	-0.001	-0.000
Lead 6	0.673	0.112	0.112	0.087	-0.001	0.001	-0.001	-0.001
Lead 7	-0.001	0.000	0.000	-0.108	0.681	0.615	-0.001	-0.001
Lead 8	0.640	0.304	0.304	0.014	1.016	0.717	0.486	-0.443

Tab. B.2: P-values for the maximum of signal par., band 500-700 Hz

Signal maximum band1: p-Values	PreUP	PreDOWN	AfUP	AfDOWN
Lead 1	0.0190	0.1427	0.0315	0.2210
Lead 2	0.0107	0.7482	0.0427	0.2701
Lead 4	0.0745	0.2023	0.0663	0.1465
Lead 6	0.0245	0.6459	0.1763	0.1202
Lead 7	0.0746	0.8295	0.3231	0.3333
Lead 8	0.1525	0.0865	0.2404	0.4156

Tab. B.3: Maximum of signal, band 700-1000 Hz, h0: values come from the same distribution with adequate mean value

Difference [mV]	PreUP		PreDOWN		AfUP		AfDOWN	
	Mean	Std	Mean	Std	Mean	Std	Mean	Std
Lead 1	-0.001	0.000	0.000	-0.000	-0.001	0.000	-0.000	-0.001
Lead 2	0.717	0.486	0.486	1.324	1.179	0.550	0.701	-0.294
Lead 4	-0.001	-0.000	-0.000	0.392	-0.001	-0.000	-0.001	-0.000
Lead 6	-0.001	0.000	0.000	0.000	-0.001	0.000	-0.000	-0.000
Lead 7	0.456	0.466	0.466	0.336	0.607	0.658	-0.000	-0.000
Lead 8	1.434	0.593	0.593	-0.039	1.468	0.443	0.505	-0.152

Tab. B.4: P-values for the maximum of signal par., band 700-1000 Hz

Signal maximum band1: p-Values	**PreUP**	**PreDOWN**	**AfUP**	**AfDOWN**
Lead 1	0.0932	0.8273	0.0959	0.5268
Lead 2	0.2262	0.5513	0.1630	0.2329
Lead 4	0.0303	0.0443	0.3333	0.3333
Lead 6	0.0549	0.3333	0.0417	0.3333
Lead 7	0.4321	0.7329	0.3643	0.3333
Lead 8	0.1088	0.0087	0.0958	0.0624

Tab. B.5: Hilbert envelope width, band 500-700 Hz, h0: values come from the same distribution with adequate mean value

Difference	**PreUP**		**PreDOWN**		**AfUP**		**AfDOWN**	
[sample]	**Mean**	**Std**	**Mean**	**Std**	**Mean**	**Std**	**Mean**	**Std**
Lead 1	0.09	0.019	0.019	18.385	18.5	4.950	18.5	-0.707
Lead 2	15.5	23.335	23.335	301.227	19.0	1.414	188.0	233.345
Lead 4	11.0	15.556	15.556	21.213	0.06	0.009	74.5	127.986
Lead 6	-104.0	-173.948	-173.948	-151.321	-226.5	3.536	1.0	-21.213
Lead 7	42.5	12.021	12.021	-101.116	-82.5	-168.999	8.0	-57.983
Lead 8	-11.5	-0.707	-0.707	-1.414	-17.5	-10.607	-352.5	-164.756

Tab. B.6: P-values for the width of Hilbert envelope parameter, band 500-700 Hz

Envelope width band1: p-Values	**PreUP**	**PreDOWN**	**AfUP**	**AfDOWN**
textbfLead 1	0.0401	1.0000	0.3333	0.3333
Lead 2	0.4925	0.3333	0.0227	0.3333
Lead 4	0.5918	1.0000	0.2021	1.0000
Lead 6	1.000	0.3333	0.3333	1.0000
Lead 7	0.0522	1.0000	1.0000	1.0000
Lead 8	0.0986	0.3333	0.1776	0.3333

Tab. B.7: Hilbert envelope width, band 700-1000 Hz, h0: values come from the same distribution with adequate mean value

Difference	**PreUP**		**PreDOWN**		**AfUP**		**AfDOWN**	
[sample]	**Mean**	**Std**	**Mean**	**Std**	**Mean**	**Std**	**Mean**	**Std**
Lead 1	54.0	11.314	11.314	5.657	47.0	11.314	-130.5	-171.827
Lead 2	0.4	0.720	0.720	160.513	-7.0	-45.255	222.5	-374.059
Lead 4	-179.5	201.525	201.525	-3.536	267.5	24.749	109.0	-176.777
Lead 6	-352.5	187.383	187.383	0.029	-195.5	292.035	77.5	-133.643
Lead 7	-347.5	154.856	154.856	-67.175	-294.0	265.872	-60.0	-69.296
Lead 8	0.4	0.097	0.097	-0.054	48.0	16.971	-150.0	179.605

Tab. B.8: P-values for the width of Hilbert envelope parameter, band 700-1000 Hz

Envelope width band1: p-Values	**PreUP**	**PreDOWN**	**AfUP**	**AfDOWN**
Lead 1	0.3333	0.3333	0.3333	0.6667
Lead 2	0.5010	0.8372	0.9862	1.0000
Lead 4	0.6667	0.3333	0.3333	1.0000
Lead 6	0.3333	0.5676	1.0000	1.0000
Lead 7	0.1463	0.0627	0.2919	0.4681
Lead 8	0.1454	0.0676	0.6667	0.6667

Tab. B.9: Root mean square, band 500-700 Hz, h0: values come from the same distribution with adequate mean value

Difference [mV]	**PreUP**		**PreDOWN**		**AfUP**		**AfDOWN**	
	Mean	**Std**	**Mean**	**Std**	**Mean**	**Std**	**Mean**	**Std**
Lead 1	-0.001	-0.000	-0.000	0.081	-0.002	-0.000	-0.001	-0.001
Lead 2	-0.001	-0.000	-0.000	0.000	1.568	0.231	-0.001	-0.000
Lead 4	-0.000	-0.000	-0.000	0.000	-0.001	0.000	-0.000	-0.000
Lead 6	0.443	0.131	0.131	0.120	0.652	0.724	-0.000	-0.000
Lead 7	-0.000	0.000	0.000	0.027	0.688	0.775	1.169	-0.435
Lead 8	0.569	0.401	0.401	-0.063	0.904	0.653	0.381	-0.605

Tab. B.10: P-values for the RMS parameter, band 500-700 Hz

RMS band1: p-Values	**PreUP**	**PreDOWN**	**AfUP**	**AfDOWN**
Lead 1	0.0037	0.1337	0.0313	0.3333
Lead 2	0.3333	0.8550	0.0444	0.2709
Lead 4	0.0550	0.0890	0.0169	0.1553
Lead 6	0.0503	0.7248	0.3333	0.1292
Lead 7	0.1716	0.9076	0.3707	0.0764
Lead 8	0.2026	0.0863	0.2529	0.5444

Tab. B.11: Root mean square, band 700-1000 Hz, h0: values come from the same distribution with adequate mean value

Difference [mV]	**PreUP**		**PreDOWN**		**AfUP**		**AfDOWN**	
	Mean	**Std**	**Mean**	**Std**	**Mean**	**Std**	**Mean**	**Std**
Lead 1	1.522	-0.092	-0.092	-0.005	1.555	0.185	1.496	-0.175
Lead 2	1.511	-0.090	-0.090	0.104	1.498	0.175	1.472	-0.103
Lead 4	-0.002	-0.000	-0.000	0.000	-0.001	0.000	-0.001	-0.000
Lead 6	0.500	0.048	0.048	0.000	0.778	0.414	0.954	-0.207
Lead 7	-0.001	-0.000	-0.000	0.000	-0.001	0.000	-0.001	-0.000
Lead 8	-0.010	-0.000	-0.000	-0.000	-0.008	-0.000	-0.005	-0.003

Tab. B.12: P-values for the RMS parameter, band 700-1000 Hz

RMS band1: p-Values	**PreUP**	**PreDOWN**	**AfUP**	**AfDOWN**
Lead 1	0.3333	0.8542	0.1011	0.4952
Lead 2	0.1856	0.5643	0.1000	0.3608
Lead 4	0.0373	0.0308	0.0109	0.1381
Lead 6	0.0420	0.0964	0.0243	0.3333
Lead 7	0.3418	1.0000	0.3333	0.3333
Lead 8	0.0932	0.0268	0.0750	0.0823

Tab. B.13: Envelope maximum position, band 500-700 Hz, h0: values come from the same distribution with adequate mean value

Difference	**PreUP**		**PreDOWN**		**AfUP**		**AfDOWN**	
[sample]	**Mean**	**Std**	**Mean**	**Std**	**Mean**	**Std**	**Mean**	**Std**
Lead 1	-0.347	0.861	0.861	-3.536	1.607	0.356	-45.000	25.456
Lead 2	-26.500	7.778	7.778	0.010	-79.500	20.506	-46.500	26.163
Lead 4	-67.500	3.536	3.536	0.707	-74.000	-2.828	-78.000	4.243
Lead 6	-15.000	1.414	1.414	0.707	0.668	0.536	1.353	-0.018
Lead 7	-15.000	1.414	1.414	52.326	-34.000	35.355	-43.000	32.527
Lead 8	-8.000	1.414	1.414	-1.414	0.189	0.089	-24.500	0.707

Tab. B.14: P-values for the position of the envelope maximum, band 500-700 Hz

Maximum position band1: p-Values	**PreUP**	**PreDOWN**	**AfUP**	**AfDOWN**
Lead 1	0.6700	0.0472	0.0270	0.1481
Lead 2	0.0872	0.0068	0.0361	0.1463
Lead 4	0.0040	0.0008	0.0018	0.0028
Lead 6	0.0532	0.0002	0.2338	0.0151
Lead 7	0.0358	0.3333	0.3333	0.2219
Lead 8	0.3333	0.3333	0.2028	0.0336

Tab. B.15: Envelope maximum position, band 700-1000 Hz, h0: values come from the same distribution with adequate mean value

Difference	**PreUP**		**PreDOWN**		**AfUP**		**AfDOWN**	
[sample]	**Mean**	**Std**	**Mean**	**Std**	**Mean**	**Std**	**Mean**	**Std**
Lead 1	-55.5	30.406	30.406	-12.021	1.755	0.355	-77.5	7.778
Lead 2	-62.5	21.920	21.920	2.501	1.992	0.502	-141.5	34.648
Lead 4	15.0	35.355	35.355	-0.036	-30.000	4.243	65.0	141.421
Lead 6	-2.5	28.991	28.991	-0.707	-0.171	1.133	0.834	0.877
Lead 7	9.0	31.113	31.113	23.335	0.467	-0.180	-76.000	-5.657
Lead 8	-11.5	-3.536	-3.536	41.012	-44.500	23.335	-51.000	-24.042

Tab. B.16: P-values for the position of the envelope maximum, band 700-1000 Hz

Maximum position band1: p-Values	**PreUP**	**PreDOWN**	**AfUP**	**AfDOWN**
Lead 1	0.1701	0.3333	0.0251	0.1062
Lead 2	0.0928	0.7376	0.0355	0.3333
Lead 4	1.000	0.001	0.0136	1.000
Lead 6	0.9181	0.3333	0.8573	0.6549
Lead 7	0.7831	1.000	0.1144	0.3333
Lead 8	0.6667	0.5522	0.3333	0.3333

C TABLE OF CONTENT ON DVD

Enclosed files:
Novotna_Petra_DP.pdf

List of enclosed MATLAB scripts:
DP_WHOLE_PROGRAM.m
DP_amplitudeWidthRMS.m
DP_ClusteringFunction.m
DP_EnvelopeDuration.m
DP_maxPositionThroughLeads.m
DP_nacitani_filtrace.m
DP_PressVol_sort.m
DP_statistics_PressVol.m
DP_statisticsNew.m
DP_testovani_PressVol.m
DP_testovani.m